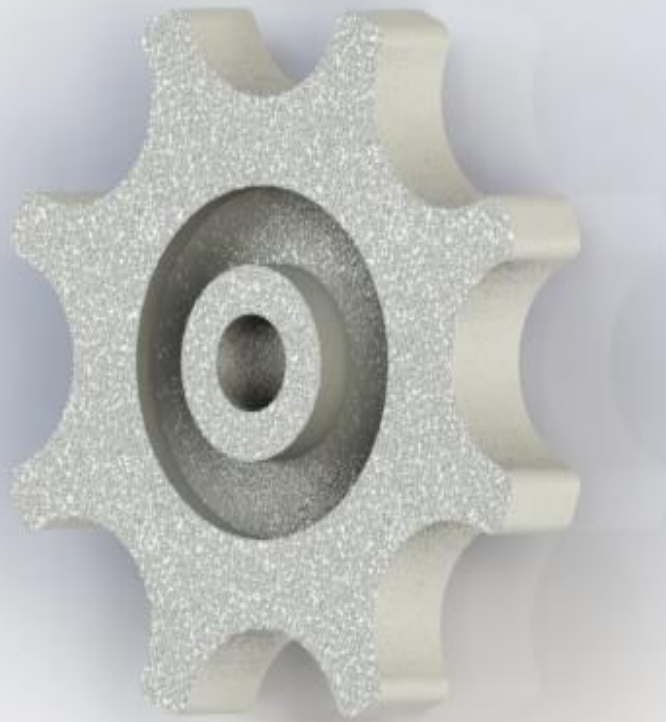


B. N. Tantuo

# Circular Reprocessing of Zamak Laryngoscope Blades



# Circular Reprocessing of Zamak Laryngoscope Blades

By

B.N. Tantuo

in partial fulfilment of the requirements for the degree of

**Master of Science**

in Biomedical Engineering

at the Delft University of Technology,

to be defended on Tuesday October 26, 2021 at 13:00 PM.

Supervisors:

Dr. ir. T. Horeman

B. J. van Straten

Thesis committee:

Prof.dr. J. Dankelman, TU Delft

Dr. ir. T. Horeman, TU Delft

B. J. van Straten, TU Delft

# Circular reprocessing of Zamak laryngoscope blades

Brian Nzieninyin Tantuo

4624742

*BM51032 TU Delft*

*Biomedical engineering, Delft University of Technology*

*(Dated: September 1<sup>st</sup>, 2021)*

There is an incentive in society to go towards a circular economy to prevent the depletion of resources and prevent climate change. The medical industry generates a large amount of waste, much of which are disposable medical instruments and consumables, of which some are not reused. In the context of creating more circularity, an “all-in-one” process has been designed for the reprocessing of the Rüsç Polaris Fiber Optic Laryngoscope Blades made from Zamak. A system was designed where blades were reprocessed by means of melting into new raw material which was used to make new products. The blades are melted in a receptacle containing a grate with 3 mm x 3mm holes which acts as a filter. This receptacle is connected to a mold where the liquid Zamak can subsequently flow into. As the holes of the filter are too small for many of the impurities to pass through, the filter prevents most non-Zamak particles on the blades from flowing into the mold along with the liquid Zamak. Multiple ingots were casted using this setup. The amount of Zamak extracted from the blades was analyzed by weighing the Zamak before and after melting. The purity of the processed material and its mechanical properties were also evaluated. Through XRF tests, it was found that the ingots had a purity of 99.6% on average in respect to 100% pure Zamak. Using the final iteration of the melting setup, the ingots were found to have an ultimate tensile strength of 223 MPa and a yield strength of 124 MPa on average. It was also possible to recover about 93% of the Zamak from the blades. To exemplify the possibility of directly creating new products with the “all-in-one” process, a rotation knob for a laparoscopic instrument named “SATA grasper” was additionally casted. The flat surfaces on the rotation knobs were grainy, while the curved surfaces were smooth. The edges of the rotation knob were sharp with a 90°C angle. After cooling down, pattern shrink was found in different sections of the rotation knobs. The shrink was not uniform and varied between 0% - 1.2% between the different sections. To achieve the previously mentioned mechanical qualities and recovery rate of Zamak, a melting temperature of 420°C was applied and the ingot mold was designed with a riser and rounded edges. It is recommended to implement these factors in the final iteration of the melting setup when reprocessing Zamak with an all-in one process. The Zamak laryngoscope blades were found to be suitable for reprocessing with the “all-in-one” process if the recommendations are followed. More widespread implementation of “all-in-one” reprocessing can contribute to higher sustainability in the medical field.

## 1. Introduction

Climate change has become an important topic of discussion in the world, leading to an increased interest in sustainability. The EU has set the objective to achieve carbon neutrality for themselves in 2050 [1]. For this to happen however, all economic sectors will need to go towards a circular economy, instead of accumulating waste. The focus of a circular

economy is minimizing waste. This can be achieved by either removing the need for (new) products or by drawing more value out of products after fulfilling their original purpose.



Figure 1. Landfill full of waste [2]

The European Green Deal is an incentive to motivate industries/economic sectors to participate in achieving a circular economy and achieve carbon neutrality [3], this includes the medical industry.

The medical industry influences the environment. The healthcare waste generation rate in high income countries varies between 1.7 kg and 8.4 kg per bed per day [4]. Hospitals have an average carbon foot print of around 5% in OECD countries, China and India [5]. The operating room and obstetric suites generate 70% of hospital solid waste [6]. As an example of the quantities of medical waste, Van Straten Medical collected over 15 tons of medical waste from hospitals in 2 months (see figure 2).

Afval Inventarisatie

Gen. Datum	Initiator	Ontvangst	Sort	Vervoerder
15-04-2021	BVS+	Maasstad 12:31	PPimpalpriet	Renewi
310 kg	20-4-2021	MeM	OLVG uit 17:53	17 Vak Laryngos CSA
205 kg	23-4-2021	BVS	Maasstad 11:05	PPimpalpriet Renewi
140 kg	05-05-2021	MeM	Maasstad 15:00	PPImpalpa Renewi
450 kg	06-05-2021	MeM	Het WkZ 11:30	1000 VAT Laryngos 3000 VAT WkZ 1 CSA
450 kg	06-05-2021	MeM	HaGa 15:00	23 VAT Main Vag CSA
155 kg	11-05-2021	Staplel	Kadband 13:00	4,5 + 11 kg Renewi
205 kg	11-05-2021	MeM	Maasstad 11:15	6200 CSA
44 kg	11-05-2021	MeM	Vision Cadabra 11:15	2 VAT CSA
120 kg	4-6-2021	Maasstad	7H 12:00	12 zakken Renewi
120 kg	23-6-2021	MeM	Maasstad 12:45	79 Impalpa Renewi
9 ton	2/7/21	Hangloot	16:00	PP Impalpa CSA
130 kg	16/7/21	Maasstad		
5 ton	8/8/21	OLVG		6200 CSA
25 kg	24/9/21	Maasstad	6:05	6 zakken CSA

Figure 2. Inventory of collected medical waste by Van Straten Medical

Hospital waste partially comes from disposable instruments. As an indication of the environmental impact of disposable instruments, Ibbotson et al. [7] made this analysis for surgical scissors. A comparison was made between reusable stainless steel scissors, disposable plastic scissors and disposable stainless steel scissors. It was found that disposable stainless steel scissors had the highest negative environmental impact. Disposables overall had a higher total cost of ownership higher than that of reusables.



Figure 3. Rüsç Polaris Fiber Optic Laryngoscope Blade

Another example of disposable metal alloy instruments used in hospitals are the Rüsç Polaris Fiber Optic Laryngoscope Blades produced by Teleflex (Teleflex, Dublin Road Westmeath, Ireland) as seen in figure 3. A laryngoscope blade is a medical instrument used to examine the interior of the larynx and for placement of an endotracheal tube. Laryngoscope blades can be made from plastic, but the laryngoscope blades by Teleflex are made from a metal alloy named Zamak. The heavier weight of Zamak compared to plastic is supposed to improve the instrument handling for the anesthesiologist. The laryngoscope blades by Teleflex are currently not reprocessed after use (see figure 4). With the goal of a circular economy in mind, a reprocessing plan will be necessary to draw new value out of the blades instead of creating more waste.



Figure 4. A bin full off used Rüscher Polaris Fiber Optic Laryngoscope Blade discarded as waste

### 1.1 Zamak

Zamak is a metal alloy consisting of mostly zinc, some aluminum and a slight amount of magnesium and copper. Zamak 3 is the most common type of Zamak and because of a lack of data on the specific material properties of the laryngoscope blade, it was assumed to be made from Zamak 3. The standard composition of Zamak 3 is 3.7-4.3% aluminum, 0.02-0.06% magnesium, a maximum of 0.1% copper with the remainder being zinc ( $\approx 95\%$ ). The function of aluminum and copper is to increase the strength and the hardness of zinc, the function of magnesium is to inhibit inter-granular corrosion [10]. The Zamak 3 standard allows for some impurities in certain concentrations, namely up to: 0.1% iron, 0.03% silicon, 0.02% nickel, 0.005% lead, 0.005 cadmium and 0.003 tin [11]. As shown in table I, it has a liquidus melting temperature of  $390^{\circ}\text{C}$  and a shrinkage factor of 1.2%.

Table I: Standard thermal and mechanical properties of Zamak 3

Zamak 3 [11]	Value	Unit
Melting Temperature - Liquidus	390	$^{\circ}\text{C}$
Melting Temperature - Solidus	380	$^{\circ}\text{C}$
Thermal conductivity	110	$\text{W/m-K}$
Specific Heat Capacity	410	$\text{J/kg-K}$
Thermal Expansion	27	$\mu\text{m/m-K}$
Viscosity [12]	$\approx 3.5@400^{\circ}\text{C}$	$\text{mPa}\cdot\text{s}$
Solidification shrinkage	1.2	%
Density	6.4	$\text{g/cm}^3$
Ultimate Tensile Strength	280	$\text{MPa}$
Yield strength (0.2% offset)	210	$\text{MPa}$
Young's modulus	86	$\text{GPa}$
Elongation at Break	11	%

### 1.2 Mold

Reprocessing of metals is usually achieved through remelting the material and casting it into a mold. When designing a mold, it is important to take into account how the part will be removed and where defects are likely to occur. See figure 5 for an example of an ingot mold. In literature, it is recommended to add a draft angle of minimally 2 degrees on the edges and corners in order to promote part release [13][14][15]. In addition to adding a draft angle, rounding of the edges is an important step to prevent stress concentrations. If the stress concentration is too high during solidification, the structural strength will be negatively affected in that area. This occurrence is especially prevalent in sharp corners and edges.

Additionally, pattern shrink should be accounted for when designing a mold. As materials expand with rising temperatures and

shrink with lower temperatures, the dimensions of your casting might become incorrect/smaller after solidification if the shrink factor is not considered in the design. When applying this to Zamak casting, the mold interior should be 1.2% larger than the intended size of the product.



Figure 5. Ingot mold containing a Zamak ingot.

### 1.3 “All-in-one” process

To incentivize reprocessing, the steps necessary to make new products from the laryngoscope blades should preferably take less effort than creating products from primary Zamak.

These steps revolve around extraction, casting and manufacturing of the material into a new product. One way of reducing the amount of steps is through an “all-in-one” process, which is defined as a process where the input is directly transformed into a desired output without needing additional active steps in-between (see figure 6). The extraction, casting and manufacturing of Zamak will occur in a single system without the user needing to continuously interact with it. By applying this concept to the laryngoscope blades, the recovery of Zamak and manufacturing of new products can sequentially be achieved. Instead of creating waste, new value can be drawn from the laryngoscope blades.

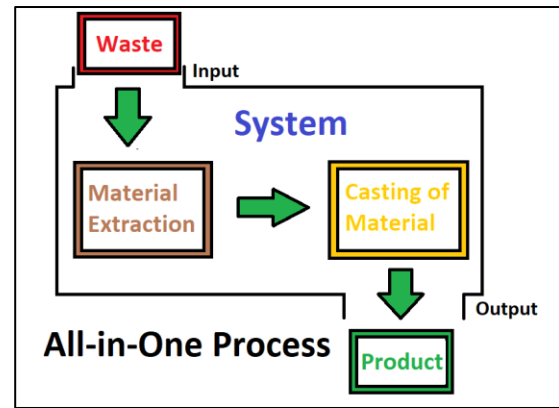


Figure 6. Schematic of the “all-in-one” process

Impurities in metals and alloys can influence the occurrence of defects and diminish material properties [8][9]. If during reprocessing the percentage of contained impurities is too high, the quality of the product will be lower in comparison to the original product, leading to downcycling. Impurities need to be mitigated as much as possible to prevent this.

For the reprocessing of the laryngoscope blades, the impurities come in the form of all the non-Zamak particles attached to the blade. The main body of the blades is made from Zamak, which is covered with an epoxy-polyester coating and contains three inserts with a diameter of 4 mm made of both stainless steel and brass. In addition to this, it contains a cylinder made of glass fiber, which is covered and held in place by a small polyvinylchloride (PVC) part. These non-Zamak particles will need to be filtered out passively where possible, while recovering as much Zamak from the blades as possible.

An “all-in-one” melting process has been designed for the reprocessing of the Zamak blades, with the goal of researching the product requirements to make a new product from Zamak. The design process and reprocessing results are discussed.

## 2. Methods

In this section the methods and tools used to perform tests and reach the design requirements will be described.

### 2.1 Reprocessing method

Preferably, the reprocessed Zamak will have similar quality compared to the original product. In order to reliably reprocess a metal, melting it down and casting it into a new shape is the primary way to achieve this. As the goal is to use an “all-in-one” process structure, the melting of Zamak needs to be conducted in conjunction with casting it, without manual operations being necessary in between.

An induction furnace (electric melting oven, KOS, electric crucible, series 219029) was used for the melting of the Zamak (see figure 7). It contained a cylindrical crucible with a diameter of 395 mm and a height of 345 mm. The temperature inside the crucible is programmable, allowing for a temperature limit to be set.



Figure 7. The induction furnace used to melt the Zamak

The furnace used does not have a movable crucible, meaning that both the melting and casting will have to happen within the furnace for an “all-in-one” process. Due to the high temperatures, electronics and many chemicals

will lose their intended function or stop functioning when exposed to high heat for an extended time, making them unusable. Moving parts are not preferable because metals and plastics will degrade and/or melt due to extended exposure to high heat, decreasing their durability and function. The system’s functions will need to work passively, meaning the user does not need to interact with the system during the melting process. Once it has melted, the flow of the liquid Zamak will be propagated into a mold by gravity, using the principle of gravity casting. Melting and casting can sequentially be achieved in a passive manner.

### 2.2 Design process

The design process was performed in an iterative manner. The initial designs and plans were first benchmark tested to gain more insight in which areas the process was sufficient or lacking, afterwards improvements were made based on the results. After the improvements were applied, the new iteration of the process was tested.

### 2.3 Temperature

Zamak becomes liquid at a temperature of 390°C, meaning that this is the minimum temperature the furnace will have to work at. The adhesion of the epoxy-polyester coating can be reduced with the burn-off method or the bake-off method [16]. The burn-off method is the heating of a coated item to 550°C - 650°C for coating removal. At those temperatures the coating starts turning to ashes. This can be utilized in combination with Zamak’s melting temperature, as it will have become liquid at this point already. Once the coating has been degraded enough, the Zamak can flow into the mold.

Similar to the burn-off method, the bake-off method degrades the coating thermally, but instead at a temperature typically around 340°C and 400°C. The coating does not get destroyed completely with the bake-off method, but instead starts flaking and forming

cracks. This process usually takes between 3 to 6 hours. Normally, the coating is mechanically removed from the product afterwards (e.g. scraping it off). Because the Zamak will already be liquid at this point, it will be able to flow through the openings formed by the flaking and cracks. This removes the need of having to mechanically remove the coating.

The inserts are made out of brass and stainless steel, which have a melting temperature of 810 °C and 1410 °C respectively [17][18]. This gives an upper bound for the melting temperature, meaning that the melting temperature during reprocessing should stay between 390°C and 810°C to keep the inserts solid and prevent them from flowing with the Zamak while liquid.

### 2.3.1 Melting temperature iteration #1 – Benchmark test

In accordance with the burn-off method, the furnace temperature was set at 650°C. The highest burn-off temperature was chosen as it led to faster removal of the coating, faster melting rate and lower viscosity of the Zamak which allowed it to flow through the coating and into the mold easier and faster.

The higher temperature leads to higher oxidation rates however. In addition to this wearing down the equipment faster, gases are released during oxidation. These gases can be absorbed by the Zamak while in its liquid form. After solidification, the gases create defects in the form of porosity within the casting, which negatively affect the mechanical qualities and durability.

### 2.3.2 Melting temperature iteration #2

In order to reduce the oxidation rate, a lower melting temperature was chosen. The recommended melting temperature for Zamak 3 lies between 395°C and 425°C [19]. Based on this recommendation, a melting temperature of 420°C was used. As this temperature conflicts with the burn-off method, the bake-off method was used instead. The effects of the lower melting temperature were analyzed through mechanical testing.

## **2.4 Zamak recovery**

A melting setup for the extraction of Zamak was designed. The design needed to contain the ability to filter out non-Zamak particles while extracting as much Zamak as possible in a passive manner. See figure 8 for the standard melting protocol that was followed

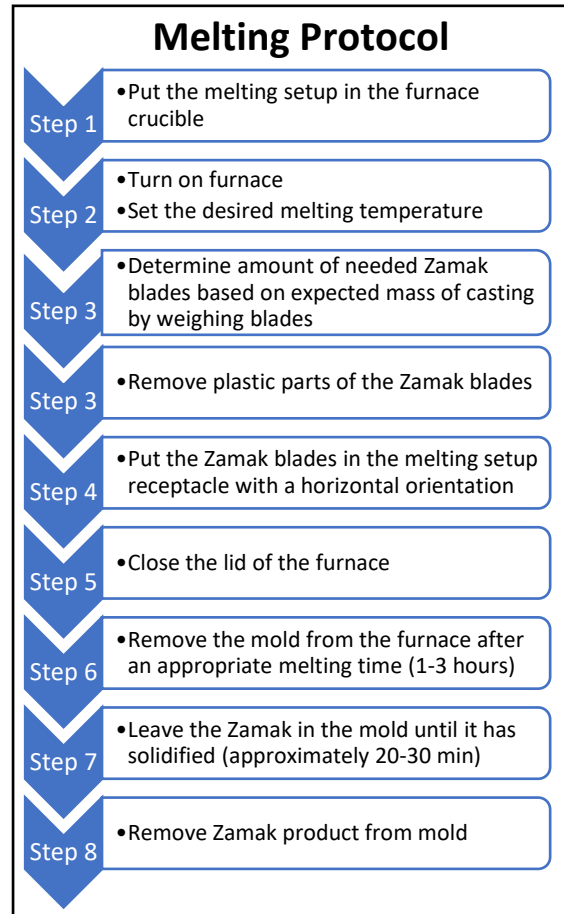


Figure 8. Melting protocol followed during tests

The amount of Zamak recovered is dependent on the run time of the furnace, where, up to a certain point, a longer run time will lead to a higher percentage of Zamak recovery. The run time of the furnace was decided empirically by visually observing when the coating had degraded enough for Zamak to flow out of the blades and when the flow of Zamak into the mold had stopped. After getting to the desired melting temperature, a visual observation by eye was made every 15 minutes to determine how much Zamak had filled the mold (see figure 9). Every observation was compared with the previous one. Not including the warm

up time of the furnace, the volume of Zamak in the mold was observed not to increase after 1 hour of melting at 650°C. At 420°C the Zamak in the mold was not observed to increase after 3 hours of melting.



Figure 9. Visual observation of amount of Zamak in mold

#### 2.4.1 Melting setup iteration #1 – Benchmark test

The first melting setup consists of a flat bottom stainless steel bowl with a grate on the bottom and a stainless steel ingot mold below it (see figure 10 and 11). The bowl's function is to hold the blades during the melting process. Once the Zamak has become liquid, it can flow through the grate, which simultaneously acts as a filter to prevent the coating residue, inserts and the particles from plastic parts to flow along into the mold. The grate has square holes square holes of 3 mm x 3 mm which prevents the inserts from falling through. The ingot mold has a square frustum shape, with a wall thickness of 1.2mm. Its inner dimensions were:

- Lower base: 140 mm x 65 mm
- Upper base: 170 mm x 80 mm
- Height: 40 mm

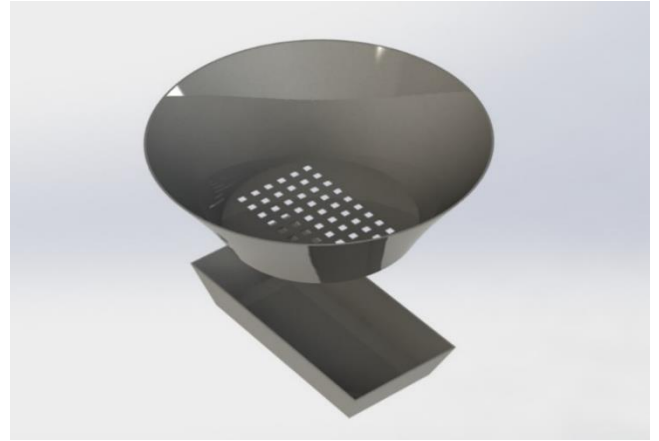


Figure 10. Melting setup #1, bowl and first iteration of the ingot mold



Figure 11. Melting setup #1, bottom of the bowl

2 Ingots were casted with this melting setup, these were named Ingot S1-A and Ingot S1-B (S1 stands for setup 1. "A","B","C", etc. denotes which ingot in the series of casted it is, where A is the first ingot created, B the second ingot, C is the third, and so on). These can be seen in figure 12 and 13. After heating the laryngoscope blades for an hour at the 650°C, the ingots were casted at the same temperature.



Figure 12. Ingot S1-A



Figure 13. Ingot S1-B

#### 2.4.2 Melting setup iteration #2

Because the bottom of the bowl from setup #1 is flat and the holes do not cover the entire bottom, some of the Zamak was trapped on sides and did not flow into the mold. Residue of this can be seen in figure 14. The second melting setup used the same principle as the first, but instead of a bowl, a stainless steel funnel and a second iteration of the ingot mold were used. The funnel is held up by a stand and has the 3 mm x 3 mm hole grate on the inner side. The mold was placed below the bottom funnel hole as shown in figure 15.



Figure 14. Zamak and coating residue in bowl from melting setup #1 sticking to the sides

One advantage of setup #2 is the conical shape of the funnel, meaning that all of the liquid inside will converge towards the funnel opening because gravity pushes it in that direction. This ensures a higher Zamak recovery in comparison with melting setup #1, as there are no flat areas in the funnel where Zamak puddles can accumulate (see figure 16). Another advantage of setup #2 is that the funnel leads the Zamak into the mold through a single hole. This helps in creating a more focused stream of into the mold and allowing molds with smaller entrances to be used compared to melting setup #1.

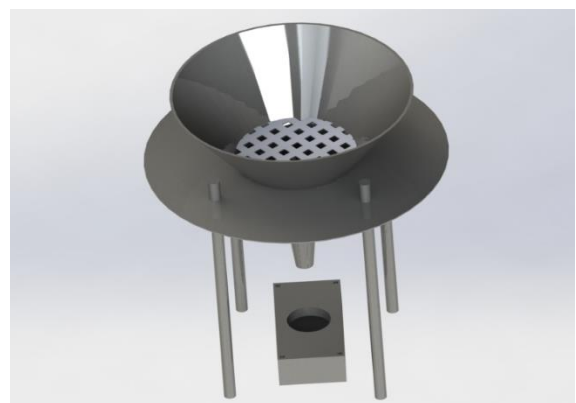


Figure 15. Melting setup #2, funnel in stand and second iteration of the ingot mold



Figure 16. Funnel used in melting setup #2

During solidification, the melt decreases its volume and the casting shrinks. The solid metal particles exert pulling forces on each other, somewhat similar to the compression of a spring. The particles are pulled in the direction where the solidification starts, which tends to start at the walls of the mold. This can cause cavities to appear (on micro and macro scale) if not enough melt is available to compensate for the lost volume. This phenomenon is called shrinkage porosity [20]. These cavities can negatively affect the mechanical qualities of the casting.

To prevent shrinkage porosity in the casting, the second iteration of the ingot mold was designed with a riser. A riser is an area in a mold that functions as a reservoir for the casting (see figure 17). The melt in the riser solidifies last and allows the casting to pull more material from the riser to fill areas where cavities would otherwise have emerged. Because of this, shrinkage porosity should only appear in the riser instead of the casting. The riser can be machined away after solidification.

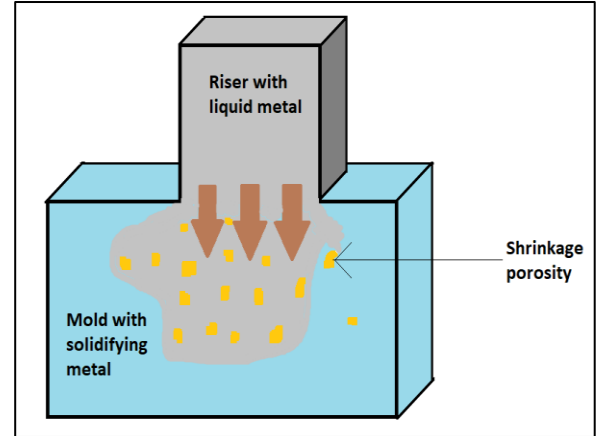


Figure 17. Example of a mold with a riser (cross-section)

The design of the riser follows Chvorinov's rule, which states that the solidification time of a casting is dependent on the relation between the volume and surface area of the casting. A casting with a large surface area and a small volume will solidify faster than vice versa [21]. The relation is written as:

$$t = B \left( \frac{V}{A} \right)^2 \quad (1)$$

Where:

$t$  = Solidification time in [s]

$B$  = Mold constant in [ $s \cdot m^{-2}$ ]

$V$  = Volume in [ $m^3$ ]

$A$  = Surface area in [ $m^2$ ]

According to DeGarmo [22], a 25% difference between the solidification time of the casting and the riser is sufficient. Because the riser and the rest of the casting use the same mold, the mold constant  $B$  would be equal to each other.

By taking this into account and applying the 25% difference, eq. (1) can be modified and simplified to:

$$\left( \frac{V}{A} \right)_{Riser}^2 = 1.25 \left( \frac{V}{A} \right)_{Casting}^2 \quad (2)$$

The mold was made out of three stainless steel slabs stacked on each other and held together by 4 nuts and bolts. See appendix A for the dimensions of the mold. The main casting had a stadium shape with a volume of  $59997 \text{ mm}^3$  and a surface area of  $20738 \text{ mm}^2$ . The riser had a cylinder shape with a volume of  $10752 \text{ mm}^3$

and a surface area of 3313 mm<sup>2</sup>. Following eq. (2), the riser will have a solidification time 26% slower than that of the casting. Because the mold and the casting will both have to cool down from the same temperature when removed from the furnace, the riser and casting solidification process will only start once the mold walls have cooled down to the Zamak solidification temperature. This means that the solidification will start at the mold walls. Assuming that every part of the mold wall cools down equally, the shrinkage cavities will appear mostly in the middle due to pulling forces working on the particles in every direction. Because of this, the riser was designed to be above the middle part of the casting so gravity will contribute to the melt flowing from the riser downwards into the casting (see figure 18 and 19).

The purpose of adding a riser was to improve the mechanical qualities of the casting by filling cavities left by shrinkage. 4 Ingots were casted at 420°C with melting setup #2 and were named Ingot S2-C, Ingot S2-D, Ingot S2-E and Ingot S2-F. To test if the riser improved the mechanical properties of the ingots, mechanical test were performed and compared with the mechanical test results of ingot mold iteration #1. As Ingot S1-A and S1-B were casted at a different temperature, Ingot S2-F was casted without riser as an indication of the effect the casting temperature has.

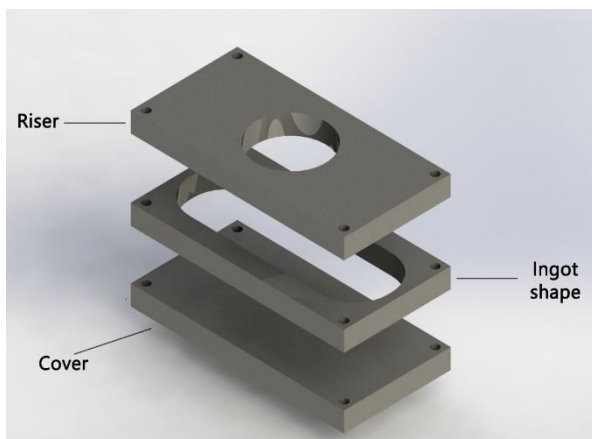


Figure 18. Exploded view of the second iteration ingot mold. Top slab: riser; middle slab: ingot shape; bottom slab: cover



Figure 19. Second iteration ingot mold

#### 2.4.3 Rotation knob mold iteration #1 – Benchmark

As an illustration of how new products can be made with the “all-in-one” process, an additional mold was made. The chosen example product was the rotation knob of a medical device named the SATA grasper (see figure 20). The SATA grasper is a modular laparoscopic instrument that allows surgeons to steer the end-effectors attached to it (scissors, graspers, etc.) during laparoscopic surgery [23]. Based on the dimensions of the rotation knob, a stainless steel mold was made (see appendix B). The mold consists of 3 slabs, each 10 mm x 55 mm x 55 mm in size, held to together by nuts and bolts (see appendix B, figure 21 and 22). The general outer shape of the rotation knob was casted, without any other details. Melting setup #2 was used, where the ingot mold was replaced by the rotation knob mold.

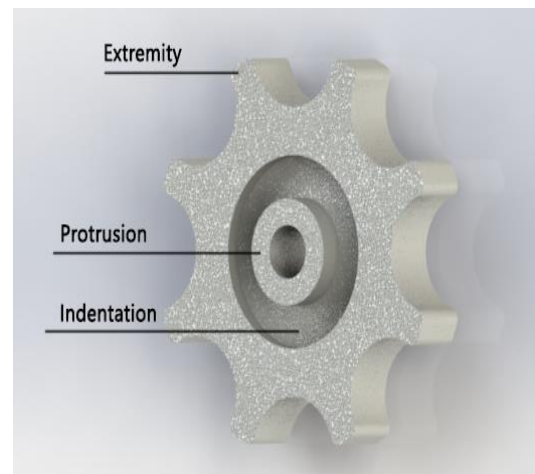


Figure 20. 3D render of the rotation knob

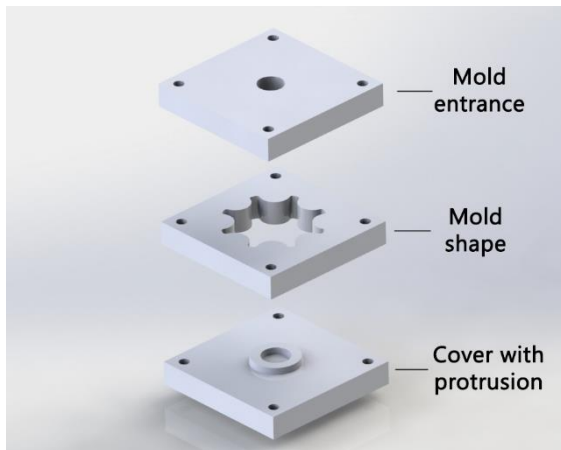


Figure 21. Exploded view of second iteration rotation knob mold



Figure 22. First iteration of the rotation knob mold disassembled

#### 2.4.4 Rotation knob mold iteration #2

The second iteration of the rotation knob mold (figure 21) has the exact same dimensions and shapes as the first (See appendix C), however, extra details in the form of indents were added to get closer to the original rotation knob.

#### 2.4.5 Measuring the rotation knobs

To determine if the shrinkage of the rotation knobs were uniform, the rotation knobs dimensions were measured and compared to the dimensions of their mold shapes. This was conducted with the Absolute AOS Digimatic caliper by Mitutoyo. The width of each extremity, protrusion and indentation were measured. The total width of the rotation knob was determined by measuring the distance between the ends of two opposing extremities. The shrinkage was determined by calculating the percentage the rotation knob dimensions

deviated from the mold shape dimensions in Appendix B and C.

### **2.5 Tools**

The melting setups were first designed with Solidworks before they were built. The rotation knob molds and the second iteration ingot mold were created with the OMAX 2652 waterjet cutter. These molds were designed in Solidworks beforehand.

### **2.6 Zamak recovery test**

The amount of Zamak extracted from the blades was tested by weighing. By weighing the amount of blades which were to be melted beforehand, and comparing this with mass of the casting, the recovery rate was determined. To get a more accurate reading, the mass of the inserts, PVC and glass fiber parts were removed. This test was performed 4 times in total. 2 times using melting setup #1 and 2 times using melting setup #2. The amount of laryngoscope blades used during each test differed due to availability at the time of testing.

### **2.7 Material composition test**

The purity of castings was analyzed by using X-ray fluorescence (XRF). Solid cylindrical samples with a diameter between 30 mm and 50 mm were needed to perform the analysis. These samples were taken from the Zamak ingots S1-A, S1-B, S2-C, S2-D, S2-E and were irradiated with high energy x-rays. When excited, all the elements in the sample subsequently emit their own x-rays with a characteristic fluorescence native to that element. By measuring these emitted waves, all the elements and their concentrations in the sample can be found. Based on the results from the XRF analysis, the purity of the Zamak samples can be derived. The purity was calculated by adding together the concentrations of zinc, aluminum, magnesium and copper in the sample. A Panalytical Axios Max WD-XRF spectrometer was used, the data evaluation was done with SuperQ5.0i/Omnian software.

## 2.8 Mechanical testing

The material properties have been tested through tensile testing and one instance of a 3-point bend test, both at a temperature of 20°C. The tensile test measures the ultimate tensile strength (UTS) of a material by recording the stress and strain applied on a material sample through tensile forces, up to its breaking point. With this data the Young's modulus and yield strength were analyzed. Based on the results from the tensile tests, stress-strain curves were graphed. The Young's modulus was determined by examining the slope in the elastic region of the stress-strain curves, the yield point was determined through the 0.2% offset method.

With a 3-point bend test, the flexural strength and maximum deformation can be analyzed. In a perfectly homogenous material, the UTS and the flexural strength would be equal. The main idea for performing the 3-point bend test in this case is to compare the UTS and flexural strength with each other, which should serve as an indication of inhomogeneity within the material. Inhomogeneity in a material is indicative of a material expressing inconsistent mechanical behavior.

Dogbone samples were used to carry out the tests, see appendix D for their design and dimensions. The dogbone samples were designed in accordance with the ASTM E8 standard [24]. They were created by first milling the Zamak ingots according to the designed dogbone shape in appendix D and afterwards sawing them in slices. An example of the created dogbone samples can be seen in figure 23.



Figure 23. Dogbone samples made from Ingot S1-A

For the tensile tests, 3 samples each from ingots S1-A and S1-B were tested. For ingots

S2-C, S2-D, S2-E and S2-F, 2 samples each were tested. As the 3 point-bend test served only as an indication of inhomogeneity, this test was only performed once using 2 samples from ingot S1-A and 1 sample from ingot S1-B. The machine used for the tests was the Zwick/Roell AllroundLine (see figure 24), the data analysis was performed through Microsoft Excel. The tensile tests were performed without an extensometer or a strain gauge due to lack of availability.



Figure 24. The Zwick/Roell AllroundLine machine used for mechanical testing

### 3. Results

Multiple tests were performed pertaining the extraction, purity and mechanical properties of Zamak. The results will be described in this section.

#### 3.1 Zamak Recovery - Weighing tests

The amount of Zamak extracted from the blades per melting setup was analyzed and compared (see table II). Using melting setup #1, about 83% of the Zamak was recovered on average in the time span of 1 hour. It was observed that some of the molten Zamak did not flow through the filter and instead stayed to the sides of the bowl, leaving leftovers inside after solidification. With melting setup #2, about 93% of the Zamak was recovered on average in the time span of 3 hours, which indicates an increase of about 10%.

Table II. Results of the weighing test for melting setup #1 and #2

Used melting setup	Test (Laryngoscope blades used)	Zamak mass before casting	Zamak mass after casting	Zamak recovery %
Melting setup #1	Test 1 @650°C (20)	1445 g	1180 g	82.8%
	Test 2 @650°C (15)	1125 g	927 g	83.5%
Melting setup #2	Test 3 @420°C (10)	750 g	680 g	91.9%
	Test 4 @420°C (6)	445 g	420 g	94.4%

#### 3.2 Material Composition - XRF Tests

The results from the XRF tests show that while impurities are present in the castings, it mostly contains Zamak. The tested ingots S1-A, S1-B, S2-C, S2-D and S2-E had a purity of 99.0%, 99.9%, 99.7%, 99.7% and 99.5% respectively relative to standard Zamak 3 (see table III and 4). Due to possible measurement errors that can be present with machines, the total purity values have been rounded to one decimal point for more reliable values. The values for the elements have been rounded to 2 decimal points. 2 decimal points were chosen so all the

elements present in the material could be represented. Most impurities seemingly came from the coating and the other plastic parts of laryngoscope blade. This was not verified however, because it was not possible to perform an XRF test on the blades beforehand (could not be made into an appropriate sample), nor was there material composition data available. The full material composition data from the XRF tests can be found in appendix E. The ingots contained more magnesium than usual.

Table III. Standard chemical composition of Zamak 3

Standard composition of Zamak 3	
Element	Percentage
Zinc (Zn)	~ 95%
Aluminum (Al)	3.7% – 4.3%
Magnesium (Mg)	0.02% – 0.06%
Copper (Cu)	0 – 0.1%

Table IV. Chemical composition of the casted ingots S1-A, S1-B, S2-C, S2-D and S2-E

XRF test (wt%)					
Element Concentration	Ingot S1-A	Ingot S1-B	Ingot S2-C	Ingot S2-D	Ingot S2-E
Zinc (Zn)	94.28 %	96.76 %	94.97 %	95.65 %	95.72 %
Aluminum (Al)	4.58%	2.96%	4.28%	3.78%	3.62%
Magnesium (Mg)	0.17%	0.10%	0.42%	0.25%	0.10%
Copper (Cu)	-	0.05%	0.04%	0.04%	0.02%
Iron (Fe)	0.03%	0.02%	0.04%	0.05%	0.46%
Nickel (Ni)	0.01%	0.01%	0.01%	0.02%	0.02%
Silicon (Si)	0.40%	0.05%	0.12%	0.1%	0.03%
Chloride (Cl)	0.08%	0.03%	0.08%	0.04%	0.01%
Sulfur (S)	0.03%	0.01%	0.03%	0.02%	0.00%
Phosphorus (P)	0.00%	0.00%	0.01%	0.01%	-
Potassium (K)	0.03%	-	-	0.01%	-
Calcium (Ca)	0.04%	-	-	0.02%	0.02%
Fluorine (F)	0.35%	-	-	-	-
Chromium (Cr)	-	-	-	0.02%	-
Total Purity %	99.0%	99.9%	99.7%	99.7%	99.5%

### 3.3 Mechanical tests

From the results of the first round of tensile tests (see table V, figure 25 and figure 27), it can be seen that the ingots do not have the same mechanical properties as the standard properties for Zamak.

The highest UTS reached by of the tested samples of ingots S1-A and S1-B was 70% (197 MPa) of the Zamak standard, the lowest UTS was 25% (70 MPa). On average, the tested samples reached a UTS of 142 MPa, 51% of the UTS standard. The yield point and Young's modulus of the samples are substantially lower when compared to the standard mechanical properties of Zamak, about 38% and 14% on average respectively.

During the machining of ingot S1-A and S1-B for sample creation, signs of gas and shrinkage porosity were observed. The areas on the ingots containing pores/holes were avoided as much as possible during machining to prevent affecting the dogbone samples. No signs of porosity defects (pores/holes) were observed on the dogbone samples themselves after inspecting them by eye.

Generally, the flexural strength and the UTS would be the same in a perfectly homogenous material. From the test results of the 3-point bend test it can be seen that the flexural strength is higher than the UTS however (see table VI and figure 26).



Figure 25. Tensile test with a dogbone sample



Figure 26. 3-point bend test with a dogbone sample

Table V. Results of the tensile test on ingot S1-A and S1-B

Zamak Properties – Benchmark test	Ultimate tensile strength	Yield strength	Young's Modulus
<b>Tensile Test – 1st round @20°C</b>			
<b>Standard Properties</b>	280 MPa	210 MPa	86 GPa
<b>Ingot S1-A</b> (Casted @650°C)			
<i>Sample A-1</i>	192 MPa	86 MPa	12 GPa
<i>Sample A-2</i>	70 MPa	50 MPa	12 GPa
<i>Sample A-3</i>	101 MPa	61 MPa	12 GPa
<b>Ingot S1-B</b> (Casted @650°C)			
<i>Sample B-1</i>	193 MPa	107 MPa	13 GPa
<i>Sample B-2</i>	97 MPa	56 MPa	12 GPa
<i>Sample B-3</i>	197 MPa	119 MPa	12 GPa

Table VI. Results of the 3-point bend test on ingot S1-A and S1-B

Zamak Properties	Flexural Strength	Maximum Deformation
<b>3-Point Bend Test @20°C</b>		
<b>Ingot S1-A</b> (Casted @650°C)		
<i>Sample A-4</i>	331 MPa	2.18 mm
<i>Sample A-5</i>	265 MPa	0.47 mm
<b>Ingot S1-B</b> (Casted @650°C)		
<i>Sample B-4</i>	370 MPa	1.05 mm

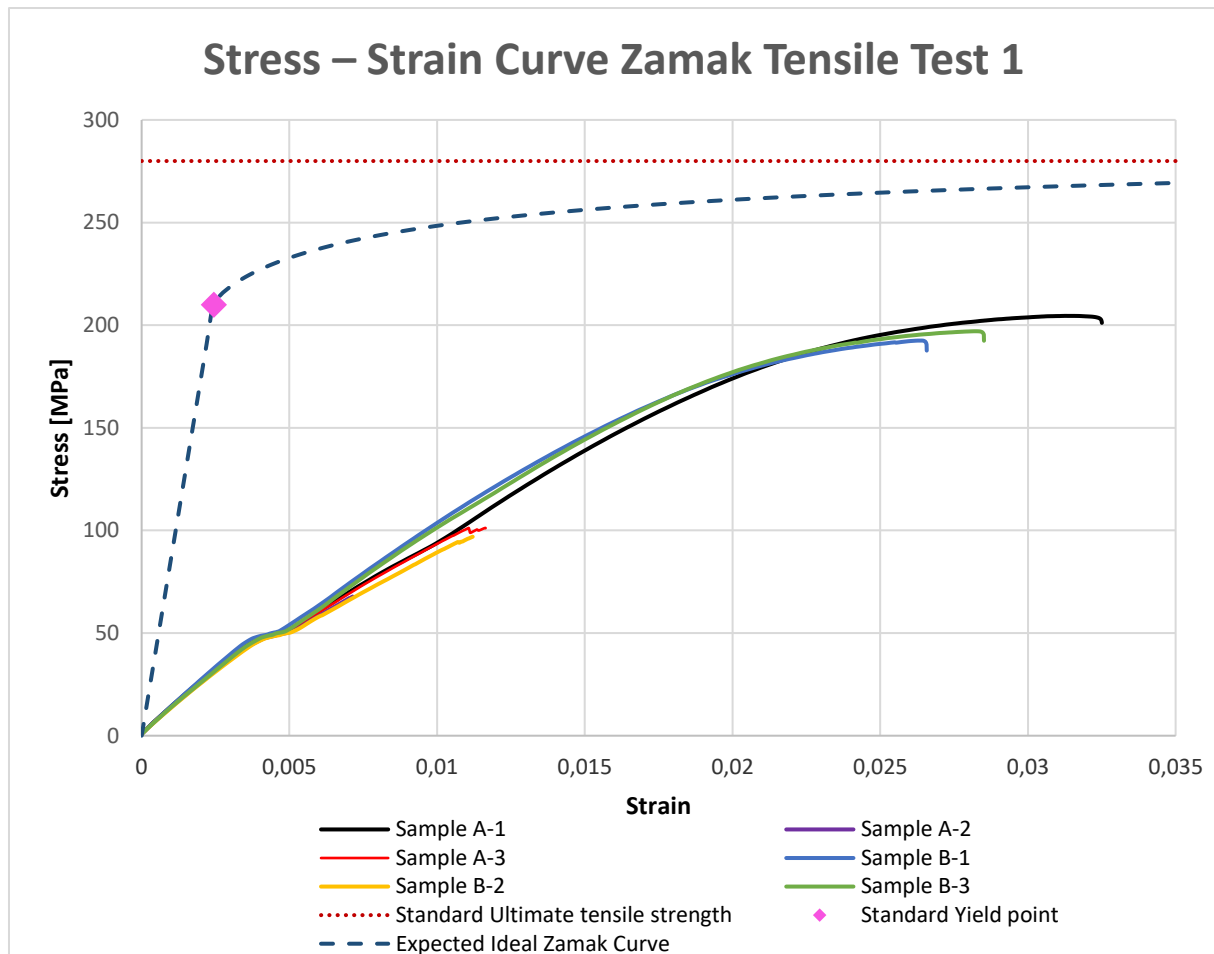


Figure 27. Stress-strain curve of the tensile test on ingot S1-A and S1-B

The highest UTS reached during the second round of tensile tests was about 109% (304 MPa) of the Zamak standard, while the lowest UTS reached was 35% (98 MPa) of the standard (see table VII and figure 28). Because ingot S2-F was casted without riser however, signs of shrinkage porosity were found on one of the samples (sample F-1). This was also the sample with the lowest UTS and yield strength. Taking only the ingots casted with a riser into account (ingot S2-C, D and E), the average UTS reached was around 80% of the standard.

The average yield strength and Young's modulus of the samples was 59% and 10% of the Zamak standard respectively. When compared to the test results from the first set of tensile tests, the second set shows an overall increase in UTS (57% increase on average) and yield strength (56% increase on average), while showing a decrease in young's

modulus (29% decrease on average). The individual stress-strain curves of each sample is available in appendix F.

Table VII. Results of the tensile test on ingot S2-C, S2-D, S2-E

Zamak Properties	Ultimate tensile strength	Yield strength	Young's Modulus
<b>Tensile Test – 2nd Round @20°C</b>			
<b>Standard Properties</b>	280 MPa	210 MPa	86 GPa
<b>Ingots S2-C (Casted @420°C + riser)</b>			
Sample C-1	220 MPa	114 MPa	6 GPa
Sample C-2	161 MPa	106 MPa	8 GPa
<b>Ingots S2-D (Casted @420°C + riser)</b>			
Sample D-1	304 MPa	182 MPa	12 GPa
Sample D-2	260 MPa	133 MPa	10 GPa
<b>Ingots S2-E (Casted @420°C + riser)</b>			
Sample E-1	210 MPa	114 MPa	8 GPa
Sample E-2	183 MPa	99 MPa	8 GPa
<b>Ingots S2-F (Casted @420°C; no riser)</b>			
Sample F-1 – contained pore defect	98 MPa	52 MPa	9 GPa
Sample F-2	184 MPa	127 MPa	9 GPa

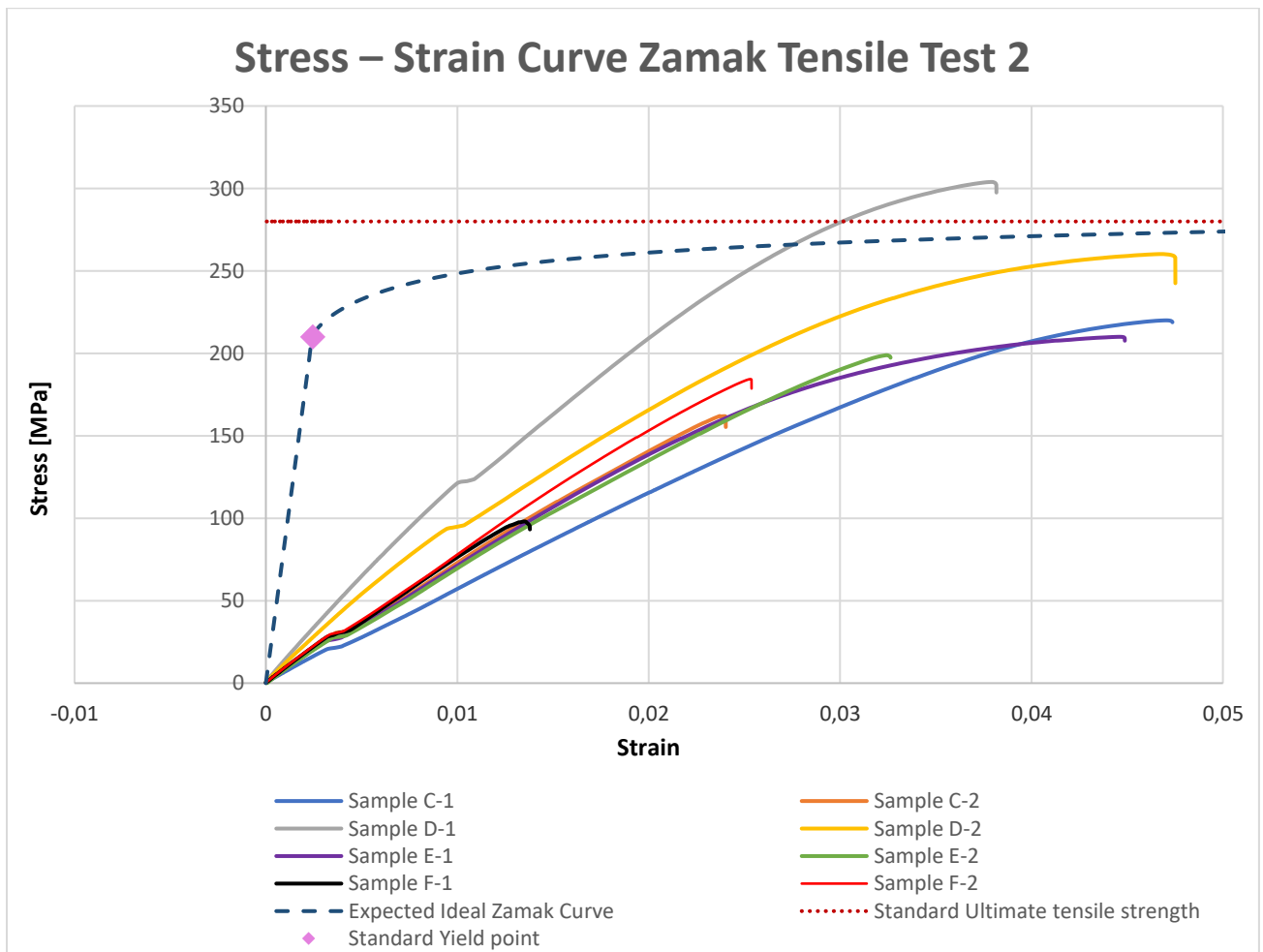


Figure 28. Stress-strain curve of the tensile test on ingot S2-C, S2-D, S2-E

### 3.4 Rotation knob

Two versions of the of the rotation knob of the SATA grasper were made (see figure 29). The first version served as an indication that the general shape was castable. The second version had retained the same shape, but had added details in the form of indentations. The castings approximate the intended rotation knob shape. The example rotation knobs were mostly made as a proof of concept, as such they were not tested functionally or mechanically.



Figure 29. Zamak castings of the rotation knob. Pictured left: first iteration; Pictured right: second iteration.

The flat surfaces of the rotation knobs had a grainy texture. The curved and rounded surfaces had a smoother texture in comparison.

#### 3.4.1 Product release

The casting made with the ingot mold of melting setup #1 could release without issues. By turning the mold upside down, the casting could fall out of the mold after it had cooled down. However, product release from the second iteration ingot mold and the rotation knob mold needed more effort. Extra force was required for part removal by means of hammering it out.

For the first iteration of the rotation knob, the mold entrance and mold shape slabs stuck together (see figure 30). The bottom cover did not adhere to the other slabs and could be separated from the rest of the mold. To completely remove the product however, it was necessary to hammer it out (see figure

31). The same thing happened with the second iteration ingot mold.



Figure 30. Top and middle mold slabs sticking together, rotation knob stuck in mold

For the second iteration of the rotation knob, the casting could not release at first because all the slabs of the mold stuck together. By fastening the top slab of the mold and holding a rod against the entrance hole, a hammer was used to apply force on it. This caused the top slab to loosen from the rest of the mold. After the top slab was removed, the other slabs were loosened in the same manner by applying force on the casting through hammering. After the slabs were separated, the casting could be obtained.



Figure 31. Rotation knob stuck in mold shape slab

#### 3.4.2 Edge sharpness

The edges of the inner mold shape were not rounded, which led to the edges of the rotation knobs being sharp. The mold shape lacks a draft angle and the edges of the mold haven't been rounded. This creates a 90° angle on the edges of the rotation knob.

### 3.4.3 Shrink

After measuring the dimensions of the rotation knobs, varying amounts of shrink was detected across the total width, extremities, thickness of the knobs, at the extremities relative to the size of their molds (see appendix B and C). This is displayed in table VIII.

*Table VIII. Pattern shrink percentages of different sections of the rotation knob*

<b>Shrink percentage</b>	<b>First iteration rotation knob</b>	<b>Second iteration rotation knob</b>
<b><i>Section of rotation knob</i></b>		
Total width	0.1% - 1.2%	0.5% -1.2%
Extremities	0% - 0.8%	0.3% -1.2%
Thickness	0.1%	0%
Protrusion	<i>n/a</i>	0%
Indentation	<i>n/a</i>	1%

In general, the shrink varied between 0% and 1.2%. The total width of the of rotation knobs had to be measured for every pair of opposing extremities, as well as the width of each individual extremity. From the results it can be seen that the amount of shrink is not uniform across every section of the rotation knobs.

## 4. Discussion

The results of the tests on the Zamak and the contribution of reprocessing on a circular economy are further discussed in this section.

### 4.1 Factors in Zamak recovery

With melting setup #1, the cutout area in the bowl does not encompass the whole bottom. This created leftover Zamak in the bowl after solidification. This explains why a lower percentage of Zamak was extracted using melting setup #1 in comparison to melting setup #2. It has been shown that by using melting setup #2, about 93% Zamak can be extracted from the blades. This Zamak can be casted into a new product while still in the furnace. Due to the amount of blades available at the time of the Zamak extraction tests, each individual test used a different amount of blades. While more Zamak is recovered using melting setup #2, a higher recovery percentage is seemingly correlated with a lower amount of blades. In comparison with the bowl of melting setup #1, no signs of leftover Zamak was found in the funnel of melting setup #2. The melting time between setup #1 and #2 also differed, but this was based on the time necessary for the coating to degrade. Because of this, it is expected that the Zamak recovery percentage for melting setup #2 will not deviate much from 93%.

### 4.2 Mechanical properties

From the tensile test results, it is noted that the mechanical properties are not guaranteed to be up to the standard. The UTS, yield strength and Young's modulus were shown to be consistently lower than the standard. There are multiple possible explanations for this.

#### 4.2.1 Casting method

One factor is the casting method. As the "all-in-one" processing method is passive in nature, gravity casting was used. When casting Zamak, die casting tends to create castings with higher mechanical properties than gravity casting [25]. This is due to the faster cooling rate,

which promotes faster solidification and in turn creates a finer microstructure. This difference is amplified in the "all-in-one" process by the fact that at the time of casting, the mold will be at the same temperature as the Zamak, meaning that there is no temperature difference between the mold and the casting to promote heat exchange. This further decreases the cooling rate.

#### 4.2.2 Impurities

Another factor which can drastically affect the mechanical qualities are the impurities [26]. The mechanical property standards of Zamak are based on almost 100% purity, where the type and concentrations of trace elements are carefully controlled. The more types and higher concentrations of impurities you have, the higher the chance of it negatively affecting the mechanical properties of the alloy and causing more inhomogeneity. Aside from nickel, iron and silicon, the rest of the impurities in the tested ingots are not normally occurring. In addition to this, the concentrations of silicon and magnesium found in the ingots was also higher than is normally added. While the extra silicon is likely due to particles from the coating and the other plastic parts, the magnesium was assumed to have already been in the blades at higher concentrations. This assumption is based on the fact that no other part of the laryngoscope blades, nor the melting setups, contain the magnesium element. This opens the possibility of the mechanical qualities of the laryngoscope blades already deviating from the standard before reprocessing.

#### 4.2.3 Defects

During machining of ingot S1-A and S1-B signs of both gas and shrinkage porosity were observed (see figure 32), no clear signs were seen on the samples however. Comparatively, no porosity was observed in ingots S2-C, S2-D and S2-E. As previously mentioned, ingot S2-F showed signs of only shrinkage porosity and sample F-1 was affected by this. Based on this, it is likely that gas porosity is lowered or prevented due to the lower casting

temperature. The effect of the casting temperature on the mechanical qualities of Zamak was not reliably verified, however, the results of sample F-2 (see table 7) does not show a large deviation relative to most of the other samples. The addition of a riser also aided in preventing shrinkage porosity from occurring. This is supported by the general increase of the mechanical qualities and lack of visual signs indicating shrinkage porosity in ingot S2-C, S2-D and S2-E. Additionally, S2-F was casted without riser and shrinkage porosity started occurring. Sample F-1 had mechanical qualities similar to the lowest results found in ingot S1-A and S1-B, possibly meaning samples A-2, A-3 and B-2 contained shrinkage porosity on microscale. This can serve as further indication that the lower mechanical qualities were caused partly by shrinkage porosity.



Figure 32. Porosity defects found after machining of Ingot S1-A

#### 4.2.4 Young's modulus

The most noticeable result of the mechanical tests are values of the Young's modulus. While it is not strange for the Young's modulus to be lower than the standard, considering the UTS and yield strength are lower as well, the Young's modulus comparatively has a higher deviation from the standard value. The tensile tests were performed without an extensometer or a strain gauge, which can help in accurately determining the Young's modulus. Considering this, the expectation is that the calculated Young's modulus is incorrect. Possibly, the deformability of the tensile test machine interfered with the measurement of the Young's modulus.

#### 4.2.5 Mechanical properties of product

The casted rotation knob model's serves as indication of the "all-in-one" process' ability to directly create a new product. While not mechanically tested, it is assumed that its mechanical properties are similar to those of the tested ingots made with melting setup #2. This assumption is based on the fact that melting setup #2 was used for the rotation knobs as well.

### **4.3 Mold**

Due to the available materials and tools, the second iteration ingot mold and the molds for the rotation knobs were created using a water jet cutter. During production, it was only possible to orient the water stream vertically and the stainless steel horizontally. Because of this, it was not possible to add a draft angle to those molds.

#### 4.3.1 Part release

The lack of a draft angle caused the castings to get stuck in the mold. Extra force had to be applied to the casting for it to release, this was done by hammering the Zamak casting to loosen and knock it out of the mold. The extra force can potentially damage the casting if too much force is used. The ingot mold for melting setup #1 did contain a draft angle which made

the removal of parts easier in comparison. After the zamak cooled down, holding the mold upside down caused the casting to fall out mold without needing to apply much extra force. This shows that a draft angle improves part release.

Applying a release agent to the mold helps in preventing the casting getting stuck by acting as thin non-adhesive barrier between the casting and the mold [27]. However, they were not used due to the long exposure of the mold to high temperatures. It was expected that a release agent would not be suitable in that case due to their potential to evaporate, combust or oxidize. This has not yet been tested however

#### 4.3.2 Mold and casting shape

The molds for the rotation knobs showed that incorporating more details in to the mold design (e.g. indentations and protrusions) is possible when reprocessing Zamak. However, having many details can cause the product to get stuck in the mold. A more detailed product leads to a more difficult and expensive to create (permanent) mold and can hinder in adding a draft angle to the mold.

While detailed castings can be made, the geometry of the mold needs to take into account how the mold separates after solidification of the casting. If a mold needs to be made for a casting with a complex shape, it would be easier for production and part release to make the mold from multiple parts (cores and cavities) instead of from one piece. The more complex your casting shape is, the more parts your mold likely needs.

Detailed castings can be divided in multiple sections (e.g. main body, protrusions, indentations, castings with asymmetrical shapes, etc.) and will have cooling rates in different sections due to the differing surface areas and volumes. Pattern shrink occurs due to thermal contraction, where materials tend to shrink when the temperature lowers. As the cooling rates can differ, this can also lead to

non-uniform shrinkage, as was measured in the castings of the rotation knobs.

Castings with sharp corners and edges can be made, as was seen with the rotation knobs. However, it is still preferable to round them. This prevents possible stress concentrations and subsequently mechanical weakness in those sections. The presence of these issues on the rotation knobs had not been observed by eye. Because these issues weren't tested however, no guarantee can be given that they are not present.

#### 4.3.3 Sand casting

An alternative to casting using permanent molds made from stainless steel would be to use sand casting. This type of casting uses a special type of sand/clay which clumps together. By leaving a pattern imprint in the sand, sand casting allows for detailed castings to be made [28]. This pattern imprint could be created by covering the prototype of the desired product with sand and removing it afterwards for example.

Because the sand is less rigid than stainless steel and can more easily be broken apart, this would also aid with part release after casting as the part would likely not get stuck in the mold. The majority of the sand is reusable after casting as well. The effect the high temperatures inside the melting furnace will have on the sand mold has not been tested yet however.

#### **4.4 Circular economy**

Circular economies are focused on the 3R principles of Reduce, Reuse and Recycle. Reducing the usage of resources will have the largest impact on waste minimization, because it lowers the potential amount of waste that can be created in total. Reusing products extends their life cycle, prolonging the time it takes for a product to turn into waste. Recycling is focused on the end of a products life, where it has lost its intended function and the materials are reprocessed for a different purpose.

Recycling is incentivized by making it part of the business model. Ranta et al. found that Dell's circular economy business model uses recycled plastics to produce their products because this saves in material costs and increases their sustainability [29]. Applying the effects of this business model to the Zamak laryngoscope blades, reprocessing them can lower material costs for the production of medical instruments and contribute to increasing the sustainability of the medical field.

## 5. Conclusion and recommendations

A circular process has been designed which allows for the Rüscher Polaris Fiber Optic Laryngoscope Blades to be reprocessed and subsequently be turned into a new product. It is recommended to use melting setup #2, casting at 420°C and a 3 hour melting time, seeing that this yielded the best results in terms of Zamak recovery and mechanical properties. Based on the mechanical test results and part creation, recommendations are given for product and mold design.

### 5.1 Product design

When designing or creating products made from the melted Zamak blades, based on the test results, the following factors should be taken into account during design and use of the product:

- Unless used for decorative or non-structural applications, the tensile stress applied on the product should maximally be 223 MPa. Preferably, this would be lower.
- If the product is only allowed to deform elastically, the maximum tensile stress should be 123 MPa. Preferably, this would be lower.

### 5.2 Mold design

The following factors should be taken into account when designing a mold for part creation:

- Round the edges and corners of the inner mold shape to prevent possible stress concentrations.
- Incorporate a riser in the mold design. The dimensions of the riser should be dependent on Chvorinov's rule, where the riser should minimally have a 25% slower solidification time than the main casting.
- Design the mold with a draft angle of minimally 2 degrees for part release.

- If the dimension tolerances of the casting require it, take the solidification shrinkage of 1.2% into account when determining the shape and dimensions of the mold by making the mold interior 1.2% larger than the intended product size.

### 5.3 Future research

Mold separation for part release can potentially be improved by applying a release agent to the mold before casting. Using sand casting as an alternative casting method might improve part release, while simultaneously allowing more complex shapes. These adjustments can potentially be tested in future versions of the "all-in-one" process.

### 5.4 Contribution to minimizing waste

To go towards a circular economy where waste is minimized, reprocessing of products becomes an important part of a product's life cycle. Due to the amount of steps involved and the possible costs involved, the incentive to reprocess products by the end users can be low. The "all-in-one" process simplifies reprocessing so waste is turned into a new product within a single system. Due to being able to directly create a new product for the user and this process being simplified, the incentive to reprocess products at the end of their life cycle will increase. By turning waste into new raw materials, it can also save in costs when creating newer products. It has been shown that setting up an "all-in-one" process is possible and feasible in terms of reprocessing of materials and creating new products. In this case, it has been tested with a limited amount of the Zamak laryngoscope blades, which were able to be melted and casted into new shapes in a single system. By increasing the size of the system (melting setup + mold) more waste can be reprocessed at a time when upscaling. In the future, "all-in-one" reprocessing could be extended to multiple medical instruments and materials to help minimize hospital waste and create new value.

## References

- [1] Rijksoverheid Nederland. *Klimaatbeleid*. Accessed on July 2nd, 2021  
<https://www.rijksoverheid.nl/onderwerpen/klimaatverandering/klimaatbeleid>
- [2] European Parliament (2018, April 18). *Circular economy: More recycling of household waste, less landfilling*. Accessed on August 31st, 2021  
<https://www.europarl.europa.eu/news/nl/press-room/20180411IPR01518/circular-economy-more-recycling-of-household-waste-less-landfilling>
- [3] Rijksoverheid Nederland. *Green Deal aanpak*. Accessed on July 2nd, 2021  
<https://www.rijksoverheid.nl/onderwerpen/duurzame-economie/green-deal>
- [4] Minoglou, M., Gerassimidou, S., & Komilis, D. (2017). Healthcare waste generation worldwide and its dependence on socio-economic and environmental factors. *Sustainability*, 9(2), 220.
- [5] Pichler, P. P., Jaccard, I. S., Weisz, U., & Weisz, H. (2019). International comparison of health care carbon footprints. *Environmental Research Letters*, 14(6), 064004.
- [6] Walchak, A. C., Porembski, M. A., Lansinger, Y. C., Ruffin, R. A., Horinek, J. L., Conant, S., & Rayan, G. M. (2021). Operating room supply waste in elective hand surgery. *Perioperative Care and Operating Room Management*, 24, 100173.
- [7] Ibbotson, S., Dettmer, T., Kara, S., & Herrmann, C. (2013). Eco-efficiency of disposable and reusable surgical instruments—a scissors case. *The International Journal of Life Cycle Assessment*, 18(5), 1137-1148.
- [8] Gschneidner Jr, K. A. (1993). Metals, alloys and compounds-high purities do make a difference!. *Journal of alloys and compounds*, 193(1-2), 1-6.
- [9] Lipiński, T., & Ulewicz, R. (2021). The effect of the impurities spaces on the quality of structural steel working at variable loads. *Open Engineering*, 11(1), 233-238.
- [10] International Zinc Association. Alloy Specifications Accessed on March 5th, 2021,  
[https://diecasting.zinc.org/properties/en/alloy\\_specifications/](https://diecasting.zinc.org/properties/en/alloy_specifications/)
- [11] MakeltFrom.com. Zinc Alloys. Accessed on September 9th, 2020  
[www.makeitfrom.com](http://www.makeitfrom.com)
- [12] Valencia, J. J., & Quested, P. N. (2013). Thermophysical properties.
- [13] Schwartz, J. (2016, March 30th). *Injection Molding Best Practices: Draft Angles For Every Part*. Accessed on September 26th, 2019 <https://revpart.com/draft-angles-for-injection-molding/>
- [14] Hazenbosch, S. *How to design parts for Injection Molding*. Accessed on September 26th, 2019  
<https://www.3dhubs.com/knowledge-base/how-design-parts-injection-molding/>
- [15] The Library of Manufacturing. *Metal Casting Design*. Accessed on February 21th, 2021  
[http://www.thelibraryofmanufacturing.com/metalcasting\\_troubleshooting.html](http://www.thelibraryofmanufacturing.com/metalcasting_troubleshooting.html)
- [16] GizmoPlans. (2018, December 5th) *How To Remove Powder Coating (4 Different Methods)*  
<https://www.gizmoplans.com/how-to-remove-powder-coating/>

- [17] MatWeb. *304 Stainless Steel*. Accessed on September 15th, 2019  
<http://www.matweb.com/search/DataSheet.aspx?MatGUID=abc4415b0f8b490387e3c922237098da>
- [18] MatWeb. *Overview of materials for Brass*. Accessed on September 15th, 2019  
<http://www.matweb.com/search/DataSheet.aspx?MatGUID=d3bd4617903543ada92f4c101c2a20e5&ckck=1>
- [19] MatWeb. *Zinc AG40A (Zinc Alloy 3; Zn-4Al-0.4Mg; Zamak 3)*, Cast. Accessed on February 12th, 2021  
<http://www.matweb.com/search/DataSheet.aspx?MatGUID=bb106cf30fba409d9a18bfb7e0a2bc79>
- [20] Han, Q. (2008). Shrinkage porosity and gas porosity. *ASM Handbook*, 15, 370-374.
- [21] Askeland, D. R., & Wright, W. J. (2018). *Essentials of materials science and engineering*. Cengage Learning.
- [22] DeGarmo, E. P., Black, J. T., Kohser, R. A., & Klamecki, B. E. (1997). *Materials and process in manufacturing*. Upper Saddle River: Prentice Hall.
- [23] Surge-On. *The Steerable Grasper*. Accessed on October 13th, 2021  
<https://surge-on.eu/laparoscopy/>
- [24] Davis, J. R. (Ed.). (2004). *Tensile testing*. ASM international. p. 52
- [25] Pola, A., Tocci, M., & Goodwin, F. E. (2020). Review of microstructures and properties of zinc alloys. *Metals*, 10(2), 253.
- [26] Apelian, D., Paliwal, M., & Herrschaft, D. C. (1981). Casting with zinc alloys. *Jom*, 33(11), 12-20.
- [27] Wikipedia. *Release Agent*. Accessed on October 13th, 2021  
[https://en.wikipedia.org/wiki/Release\\_agent](https://en.wikipedia.org/wiki/Release_agent)
- [28] The Library of Manufacturing. *Sand Casting*. Accessed on October 13th, 2021  
[http://www.thelibraryofmanufacturing.com/metalcasting\\_sand.html](http://www.thelibraryofmanufacturing.com/metalcasting_sand.html)
- [29] Ranta, V., Aarikka-Stenroos, L., & Mäkinen, S. J. (2018). Creating value in the circular economy: A structured multiple-case analysis of business models. *Journal of cleaner production*, 201, 988-1000.

## Appendix A – Technical Drawings Ingot Mold Iteration #2

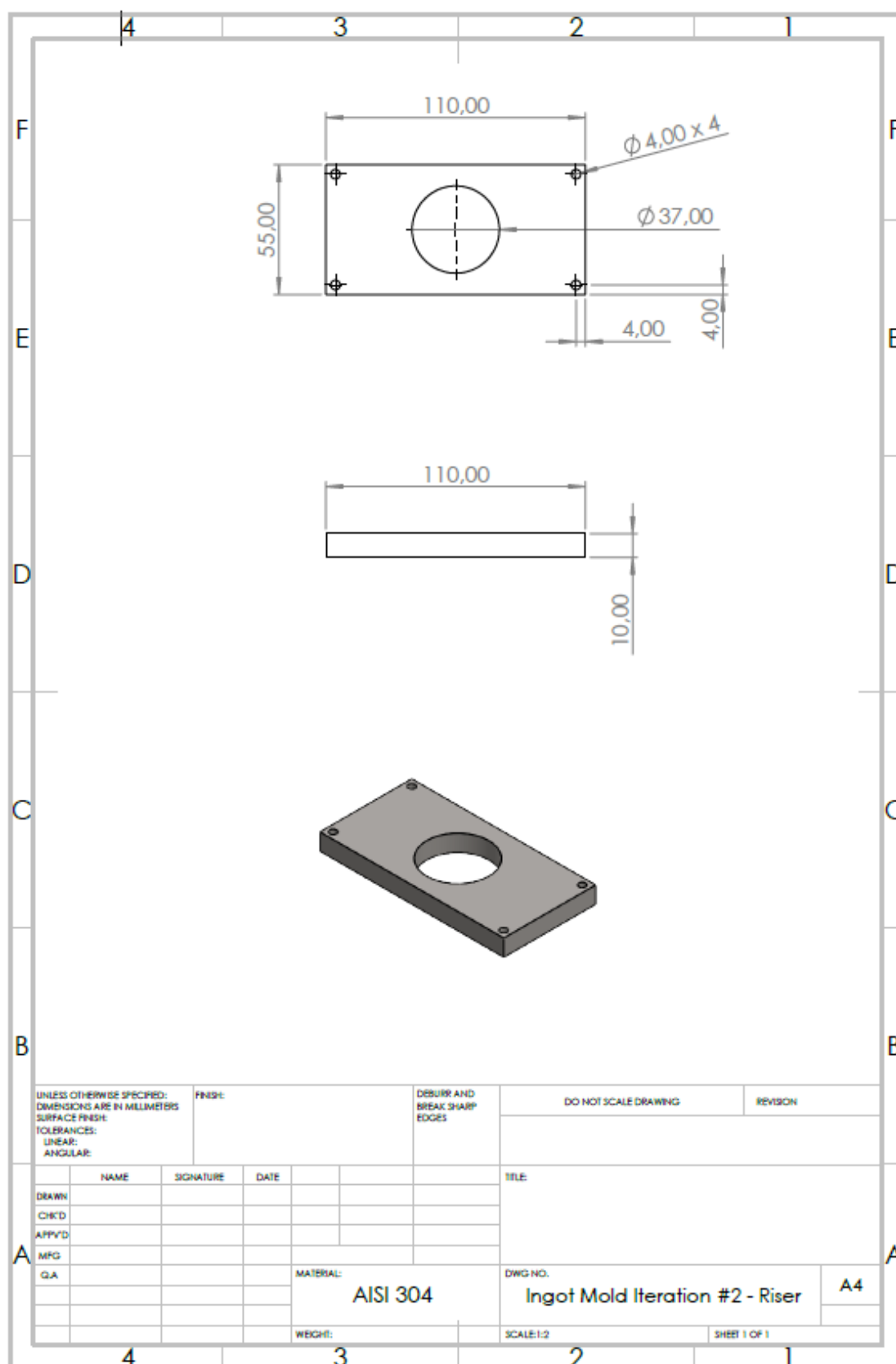


Figure 33. Ingot Mold Iteration #2 – Riser

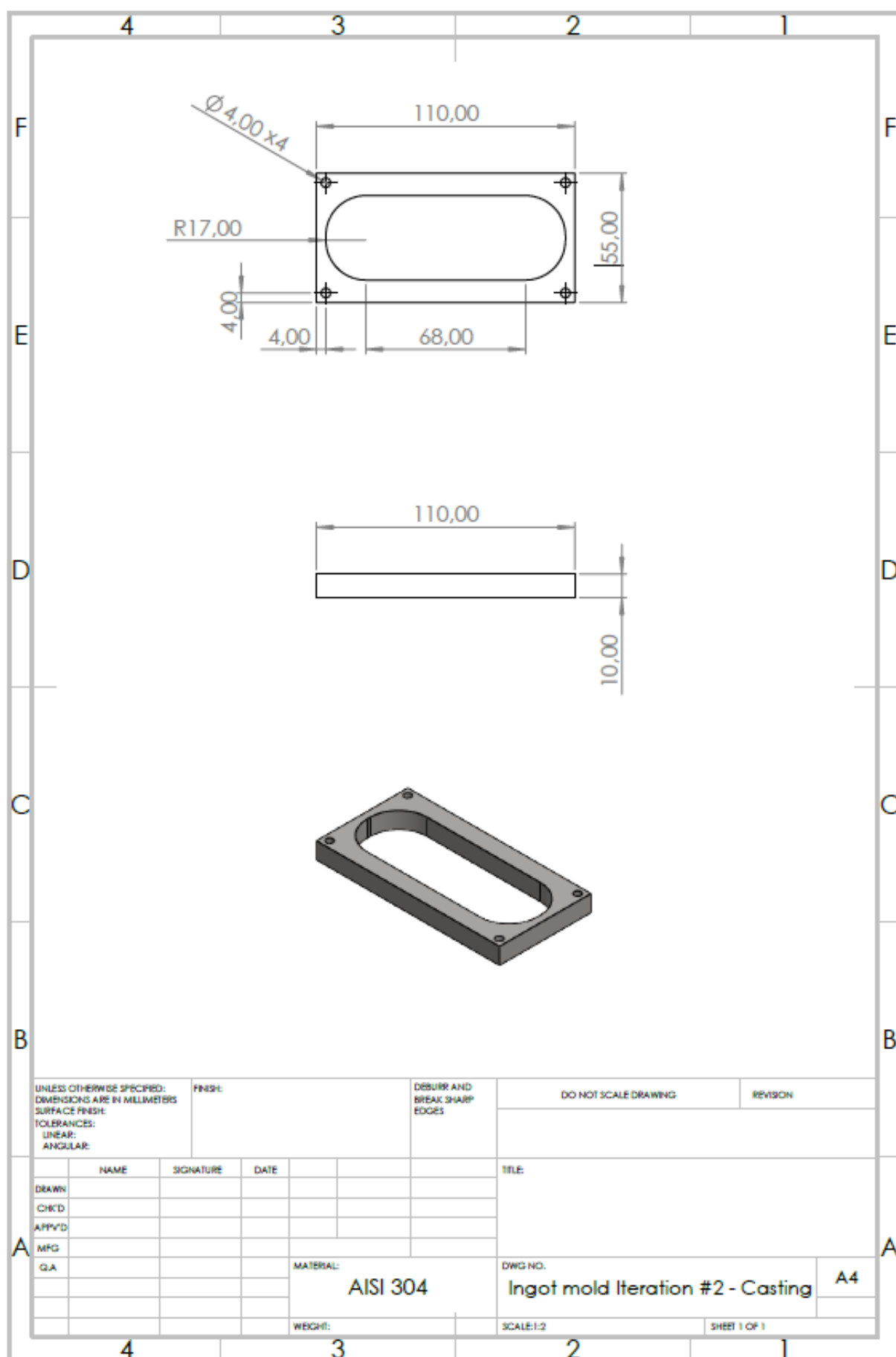


Figure 34. Ingot Mold Iteration #2 – Ingot/Casting

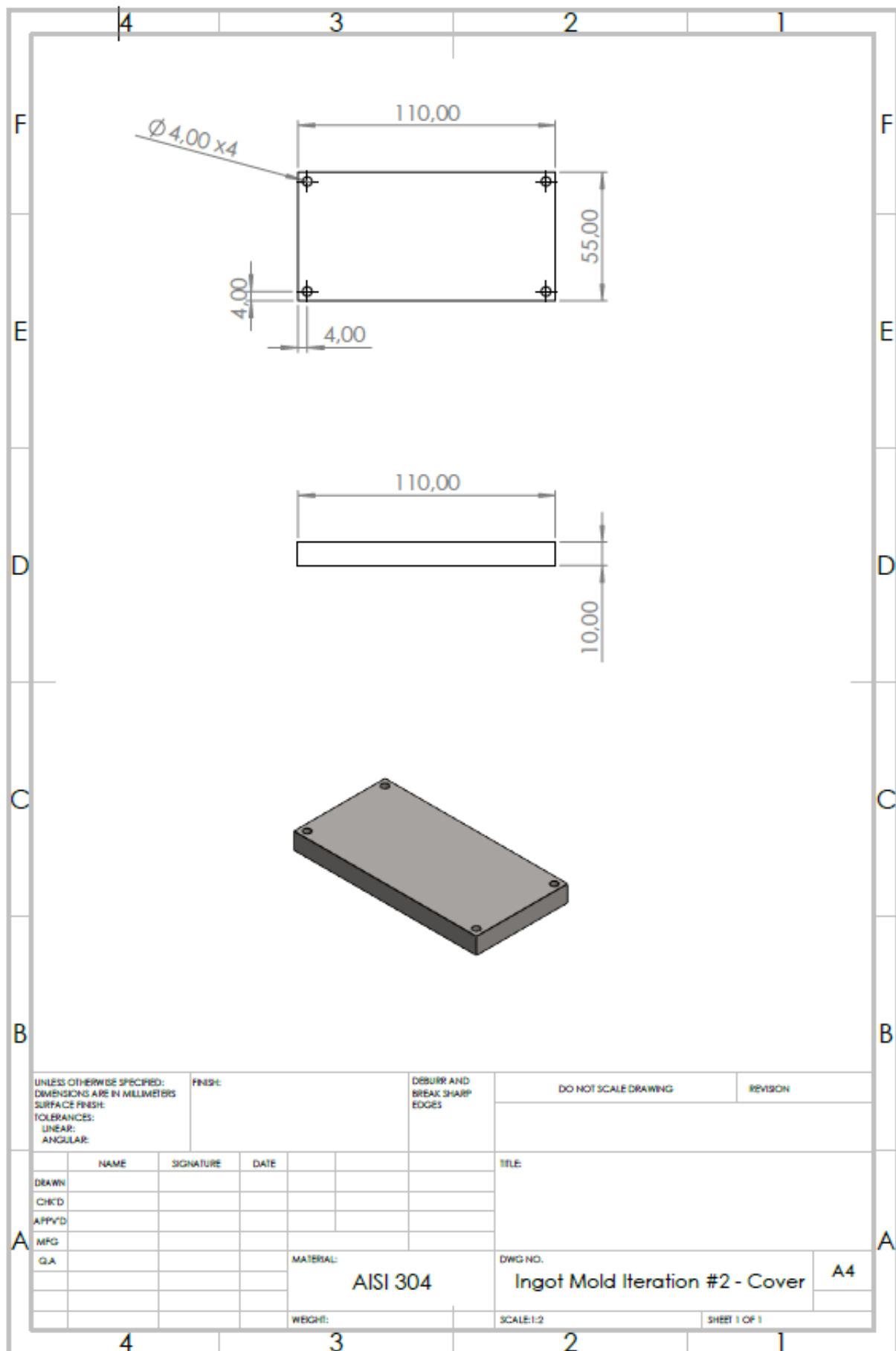


Figure 35. Ingot Mold Iteration #2 – Cover

## Appendix B – Technical Drawing Rotation Knob Mold Iteration # 1

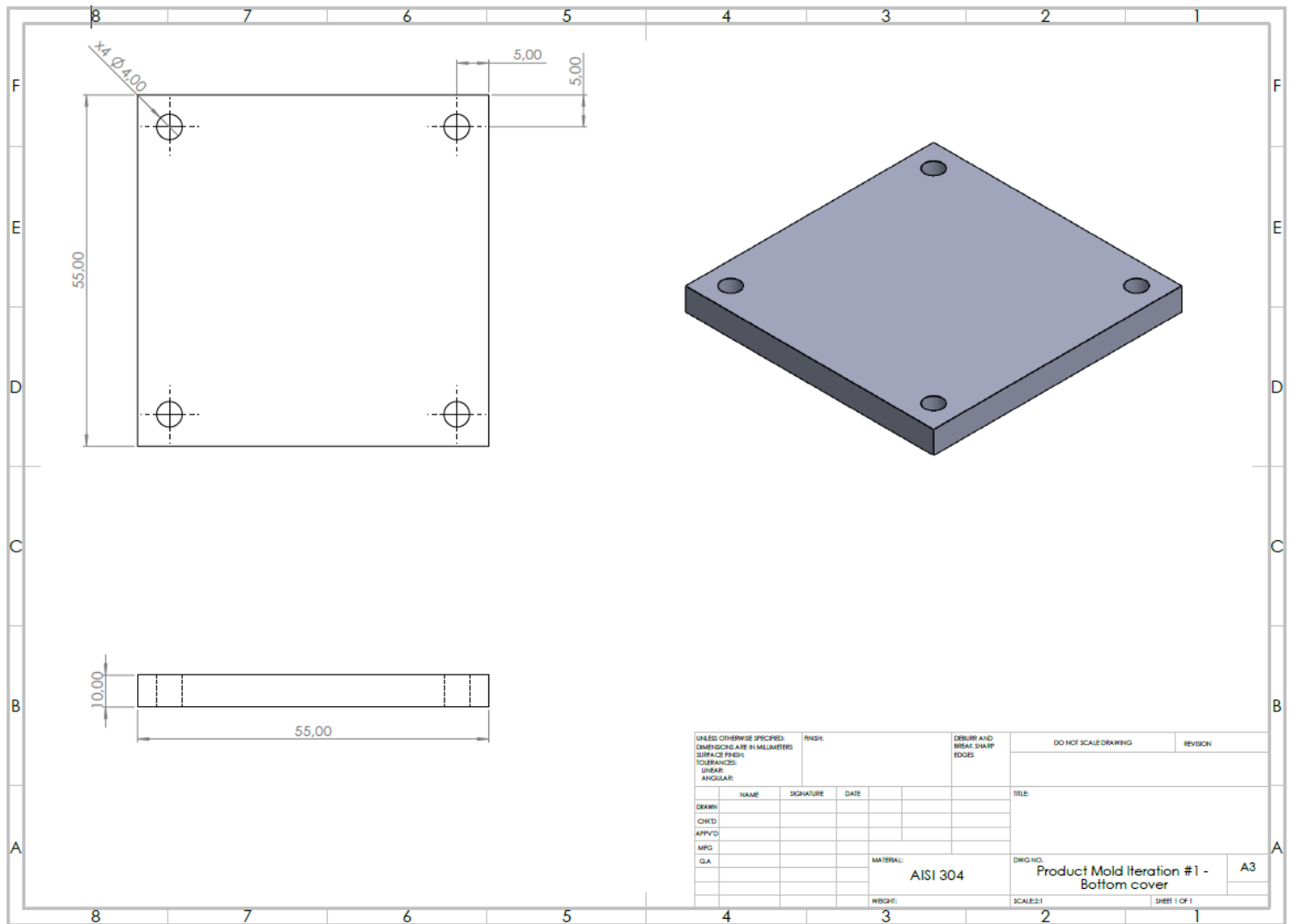


Figure 36. Rotation Knob Mold Iteration #1 – Bottom Cover

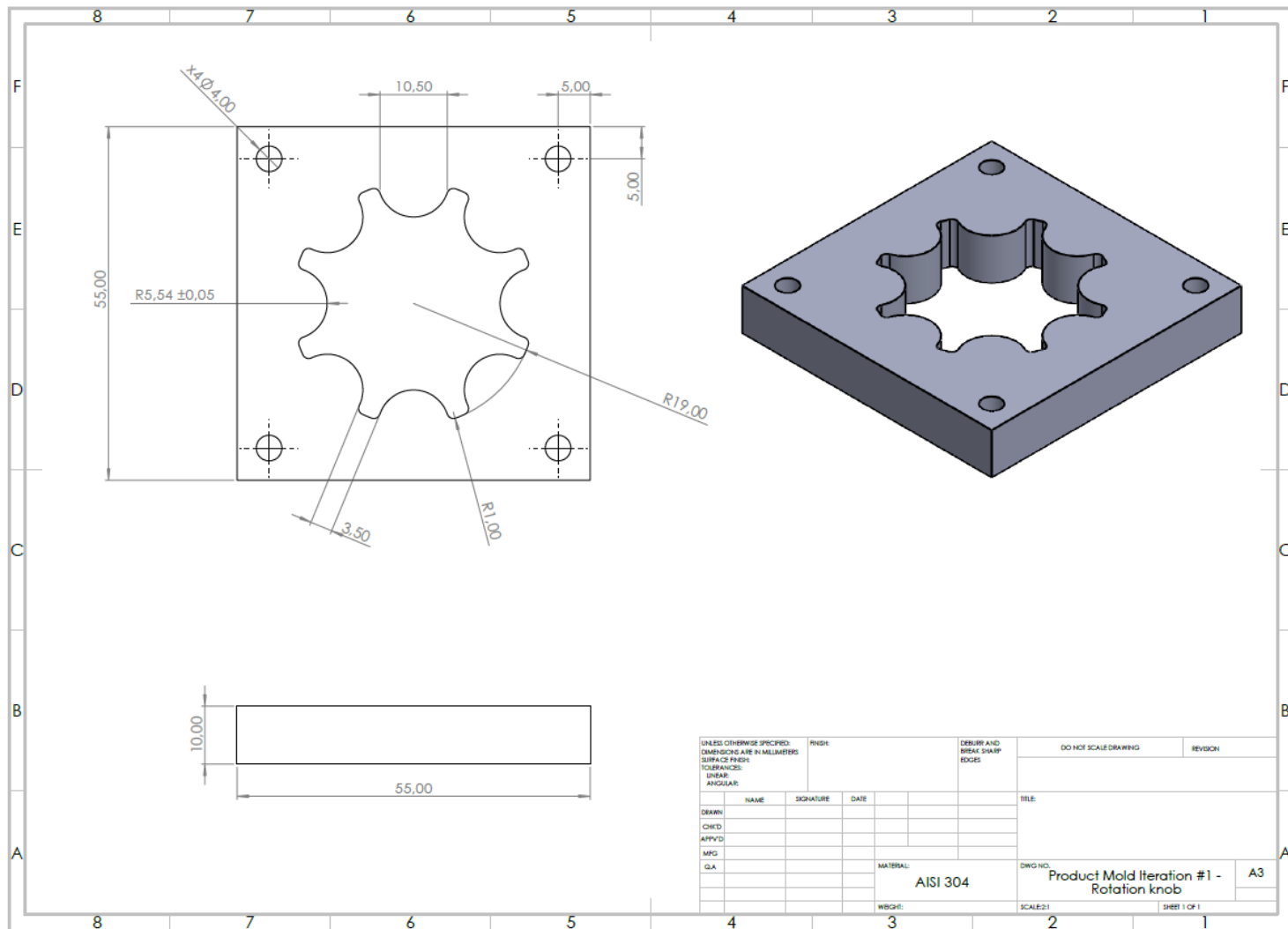


Figure 37. Rotation Knob Mold Iteration #1 – Rotation knob

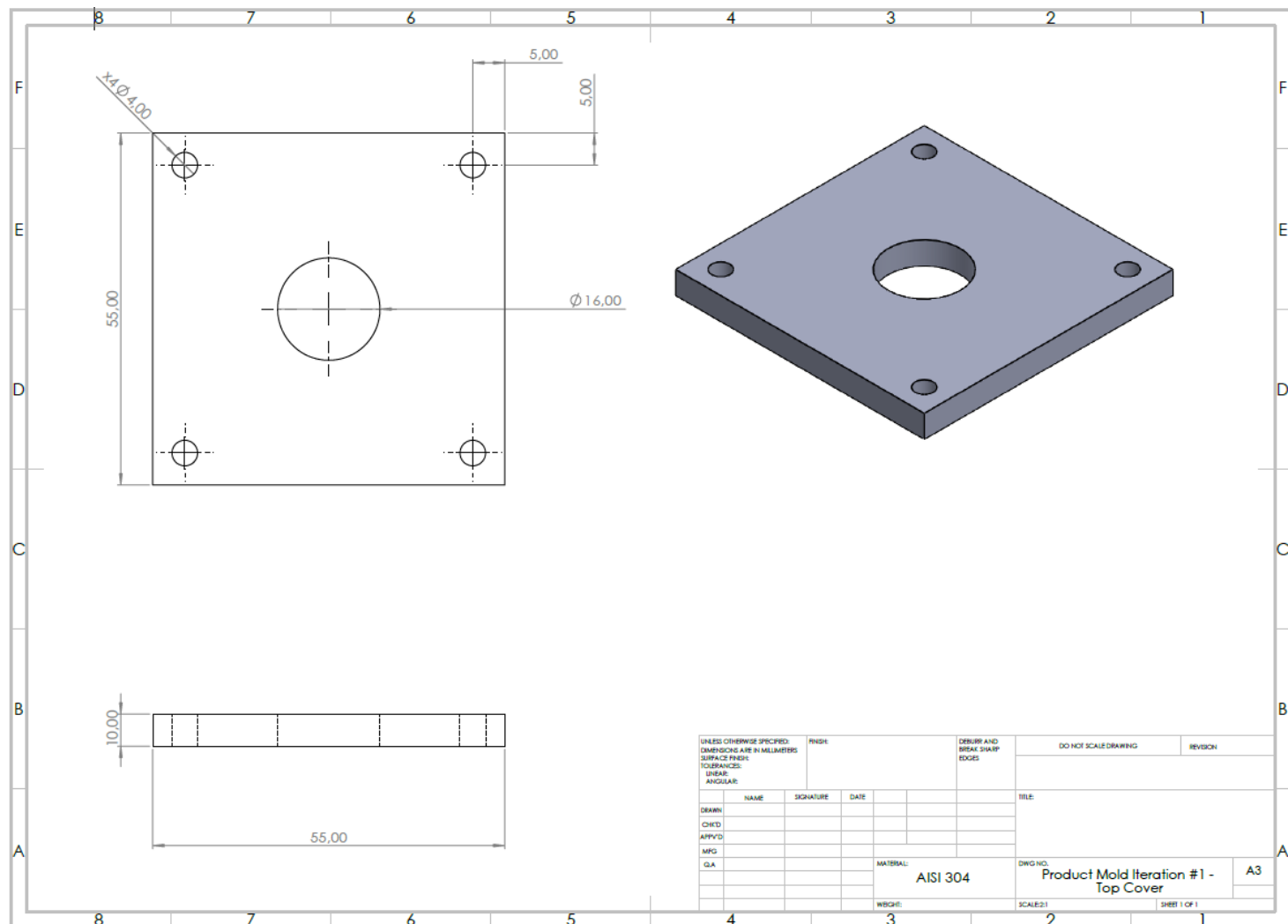


Figure 38. Rotation Knob Mold Iteration #1 – Top Cover

## Appendix C – Technical Drawing Rotation Knob Mold Iteration # 2

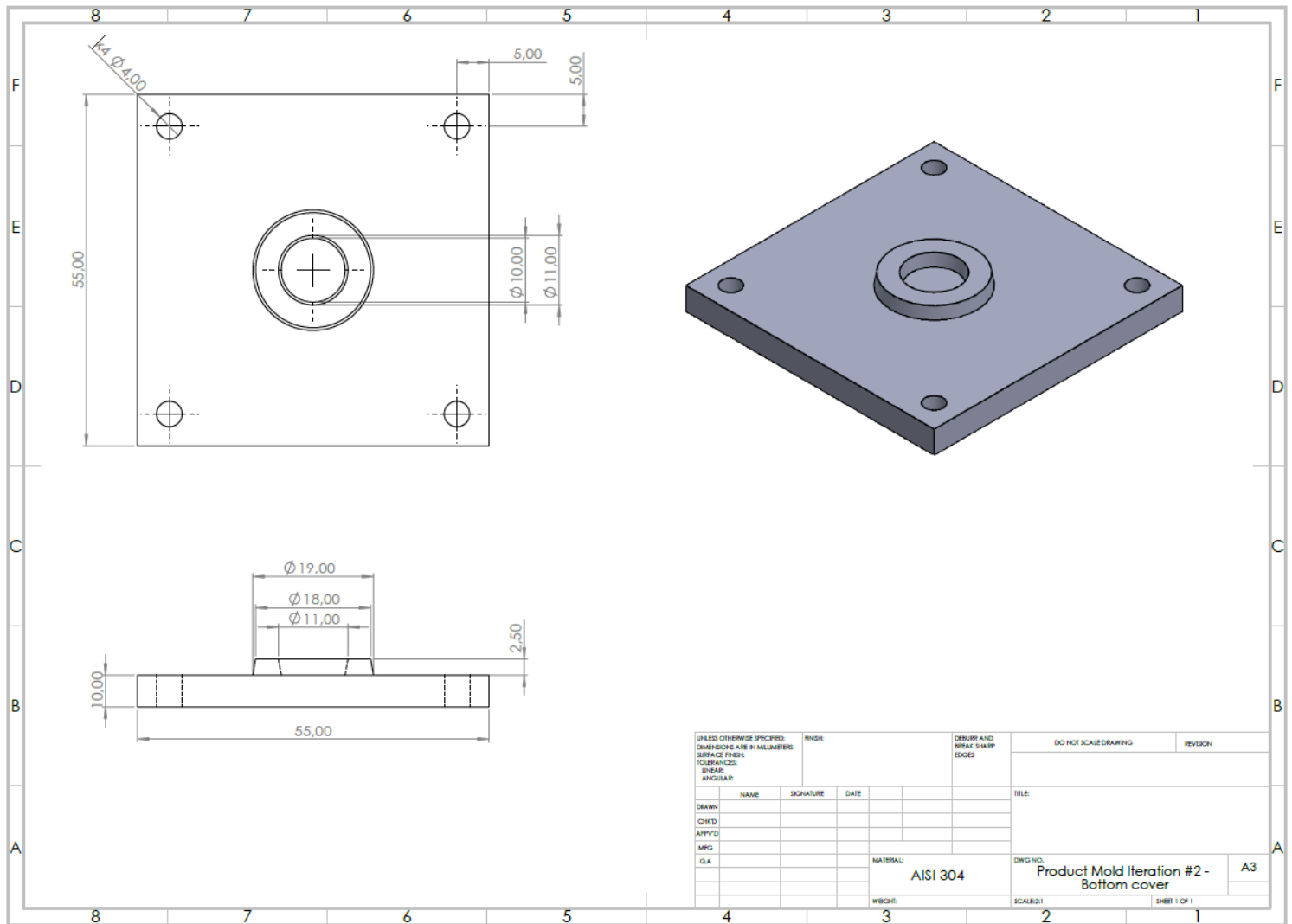


Figure 39. Rotation Knob Mold Iteration #2 – Bottom Cover

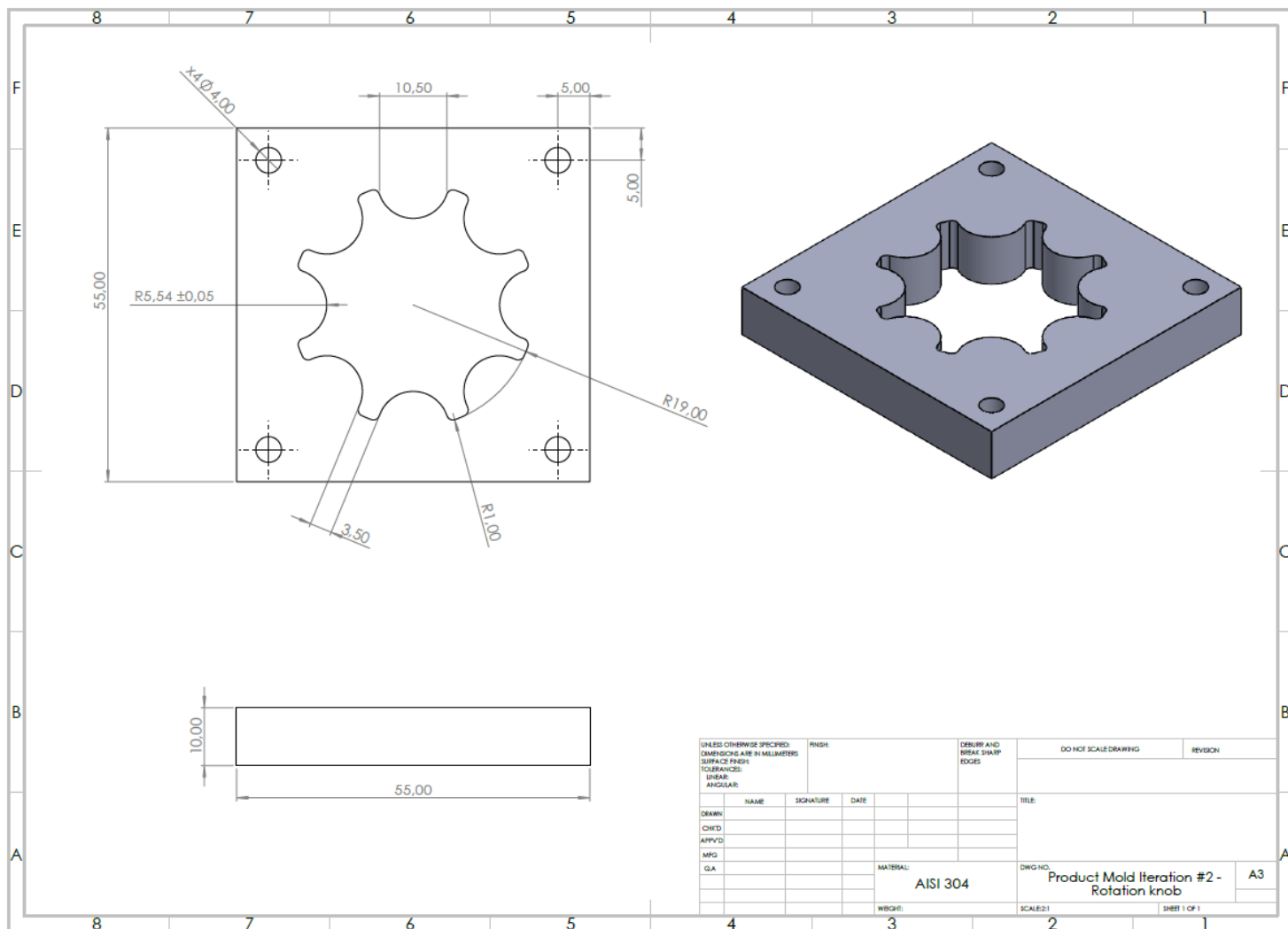


Figure 40. Rotation Knob Mold Iteration #2 – Rotation Knob

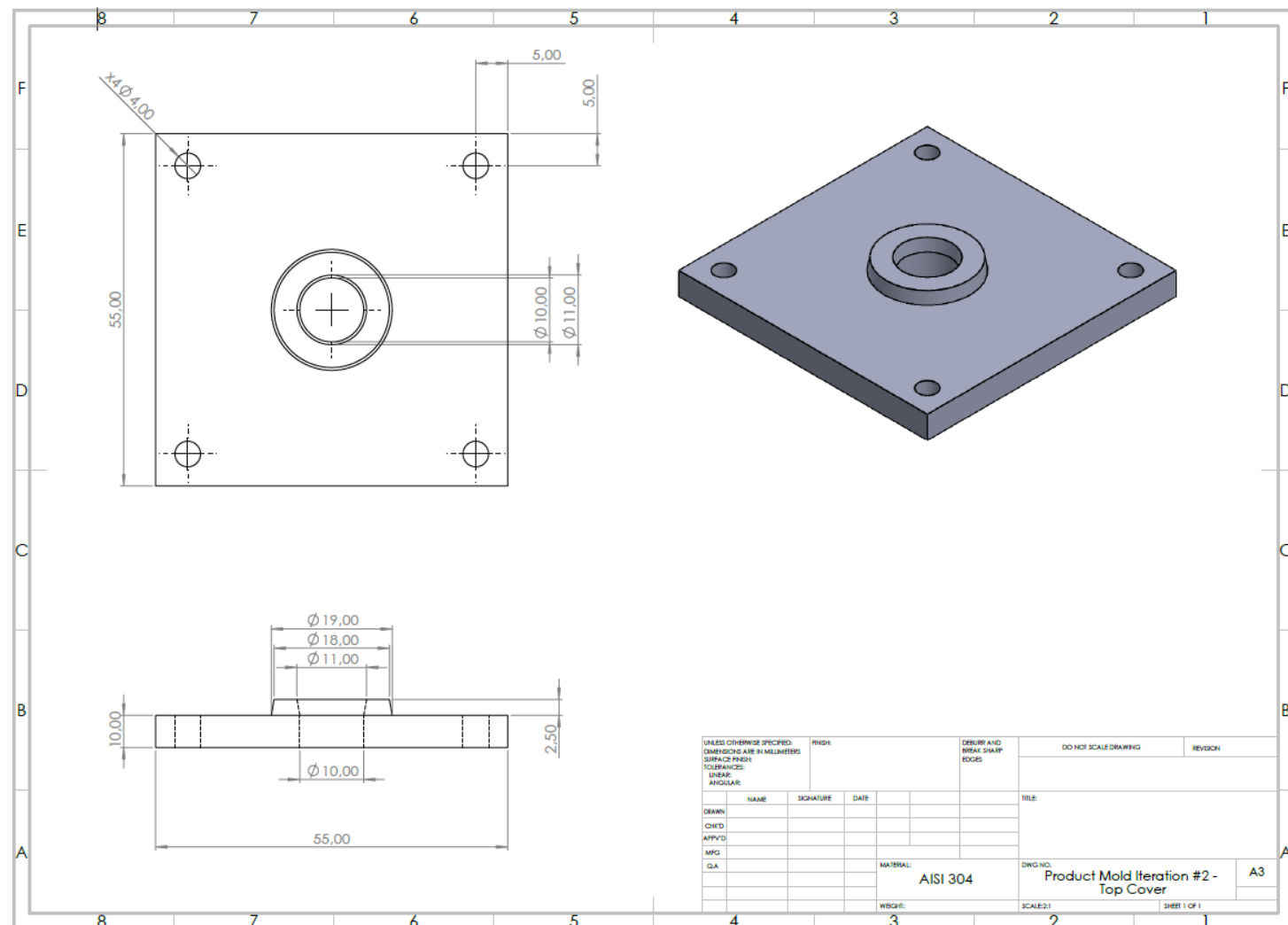


Figure 41. Rotation Knob Mold Iteration #2 – Top Cover

## Appendix D – Dogbone Sample For Mechanical Testing

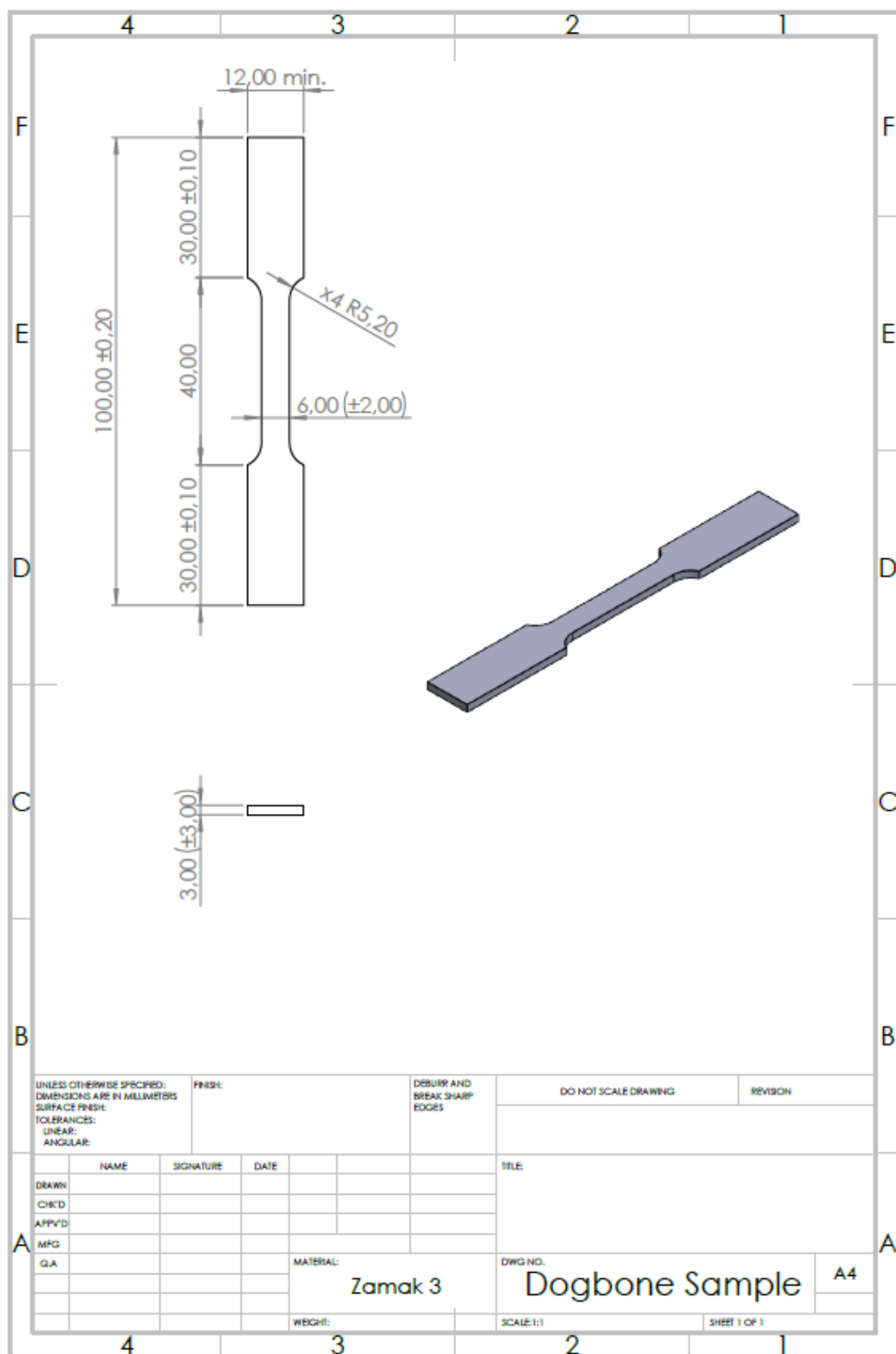


Figure 42. Dogbone Sample

## Appendix E – Test Results XRF

*Marked green are the materials that make Zamak.*

### Ingot S1-A

#### *Material composition*

	Compound Name	Conc. (wt%)	Absolute Error (wt%)
1	Zn	94.281	0.07
2	Al	4.584	0.06
3	Si	0.396	0.02
4	F	0.352	0.002
5	Mg	0.167	0.001
6	Cl	0.082	0.009
7	Ca	0.042	0.006
8	S	0.031	0.005
9	Fe	0.025	0.005
10	K	0.025	0.005
11	Ni	0.011	0.003
12	P	0.004	0.002

### Ingot S1-B

#### *Material composition*

	Compound Name	Conc. (wt%)	Absolute Error (wt%)
1	Zn	96.76	0.07
2	Al	2.963	0.05
3	Mg	0.107	0.01
4	Si	0.056	0.007
5	Cu	0.049	0.007
6	Cl	0.031	0.005
7	Fe	0.018	0.004
8	Ni	0.009	0.003
9	S	0.006	0.002
10	P	0.002	0.001

### Ingot S2-C

#### Material composition

Compound Name	Conc. (wt%)	Absolute Error (wt%)
1 Zn	94.972	0.07
2 Al	4.279	0.06
3 Mg	0.417	0.02
4 Si	0.121	0.01
5 Cl	0.078	0.008
6 Fe	0.042	0.006
7 Cu	0.036	0.006
8 S	0.034	0.006
9 Ni	0.013	0.003
10 P	0.007	0.003

### Ingot S2-D

#### Material composition

Compound Name	Conc. (wt%)	Absolute Error (wt%)
1 Zn	95.651	0.07
2 Al	3.775	0.06
3 Mg	0.254	0.02
4 Si	0.11	0.01
5 Fe	0.045	0.006
6 Cl	0.039	0.006
7 Cu	0.036	0.006
8 Ca	0.021	0.004
9 S	0.02	0.004
10 Ni	0.015	0.004
11 Cr	0.015	0.004
12 K	0.014	0.004
13 P	0.006	0.002

# Ingot S2-E

Compound Name	Conc. (wt%)	Absolute Error (wt%)
1 Zn	95.723	0.07
2 Al	3.615	0.06
3 Fe	0.455	0.03
4 Mg	0.103	0.01
5 Si	0.031	0.005
6 Cu	0.022	0.004
7 Ca	0.021	0.004
8 Ni	0.018	0.004
9 Cl	0.006	0.002
10 S	0.004	0.002

*Marked green are the materials that make Zamak.*

## Appendix F – Stress-Strain Curves Of Mechanical Test Samples

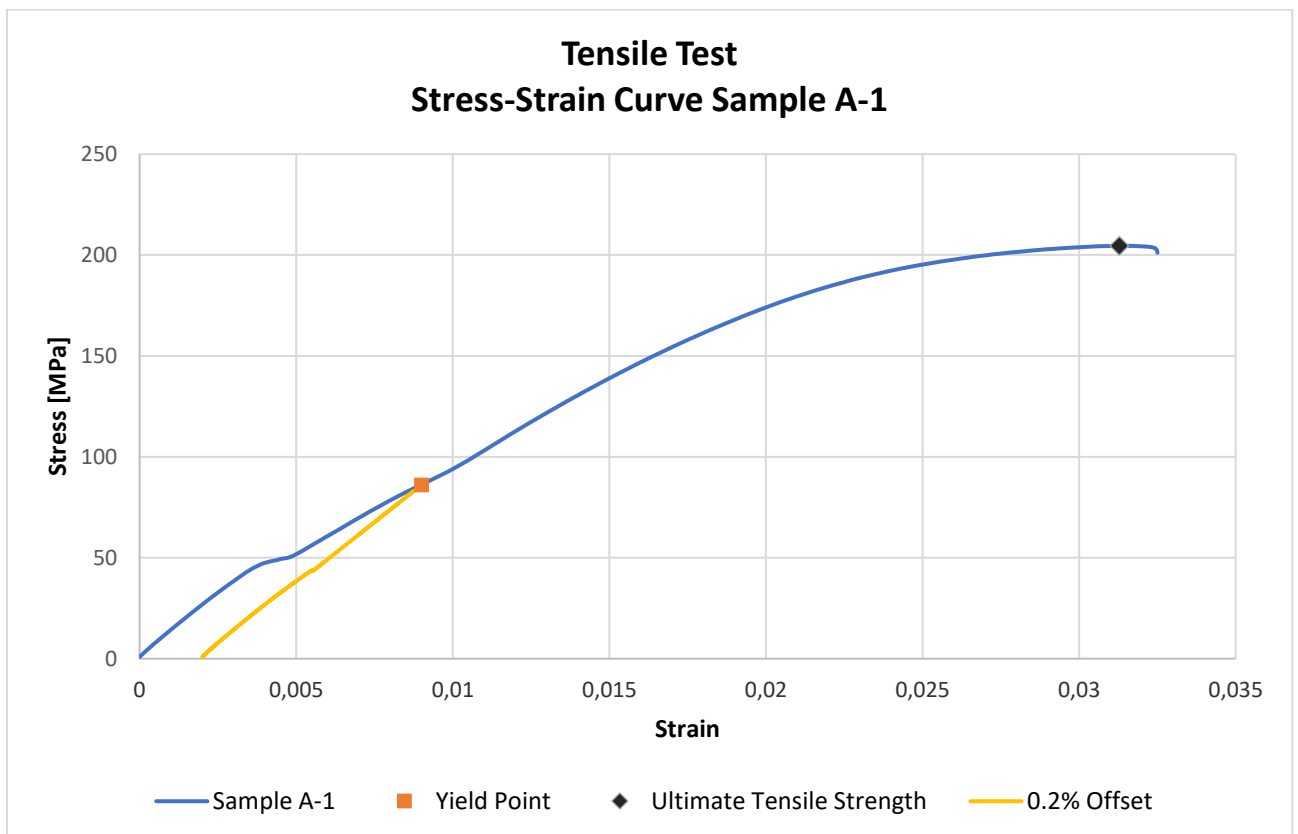


Figure 43. Stress-strain curve of tensile test sample A-1

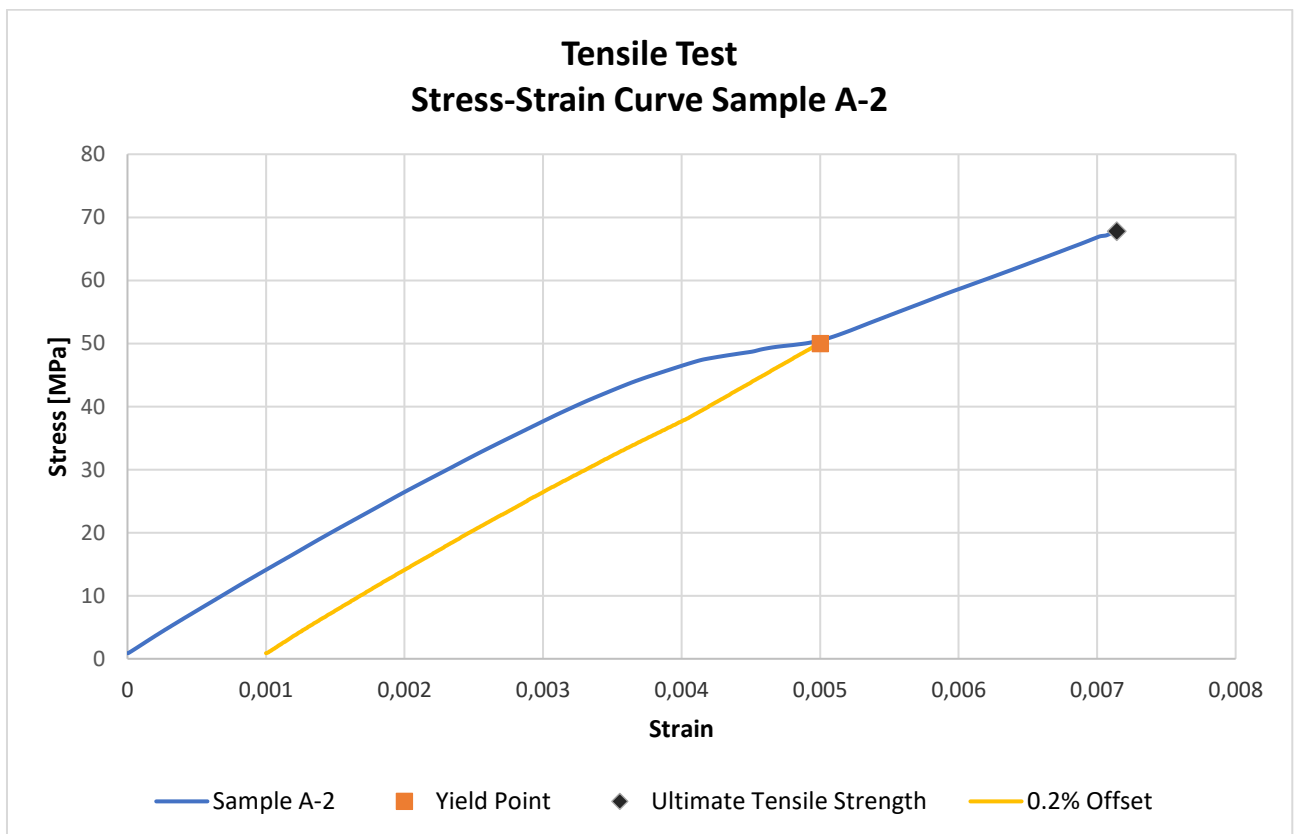


Figure 44. Stress-strain curve of tensile test sample A-2

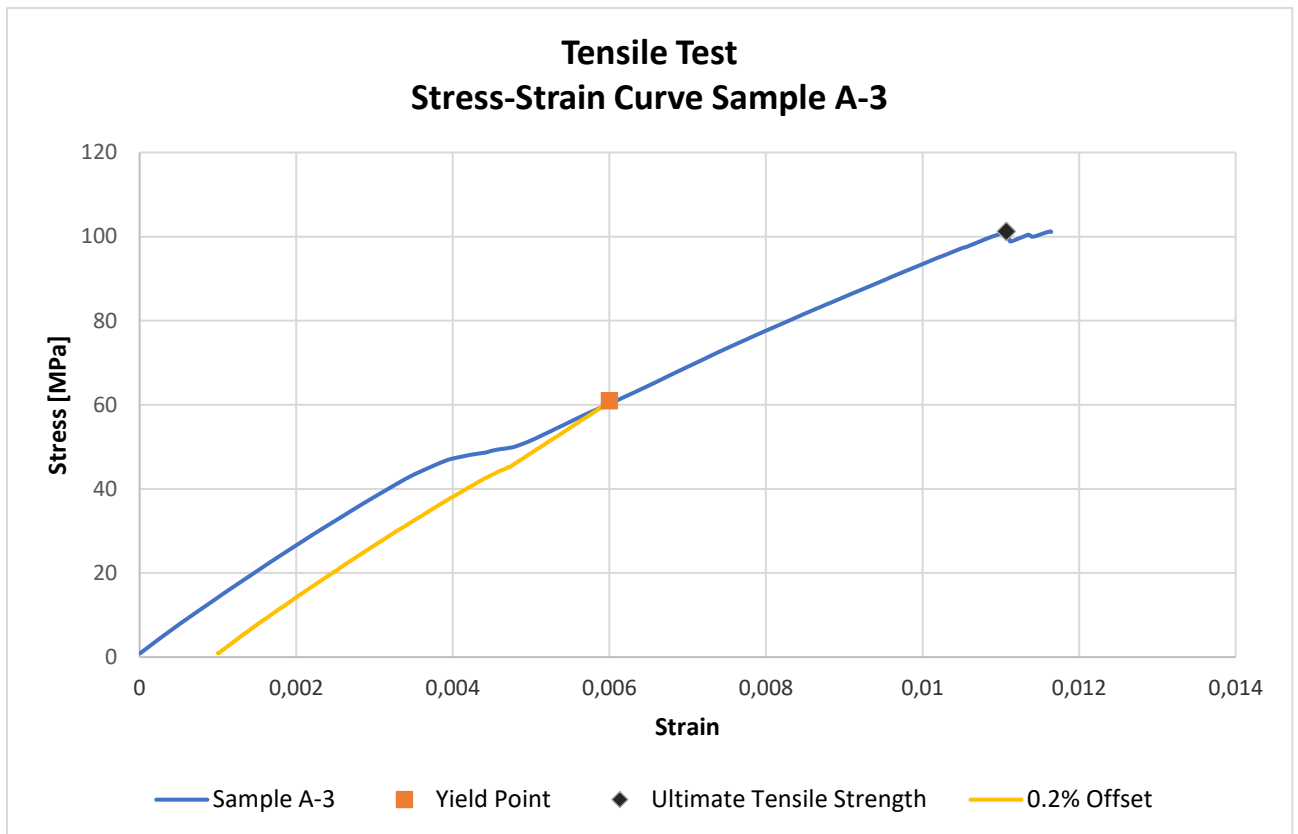


Figure 45. Stress-strain curve of tensile test sample A-3

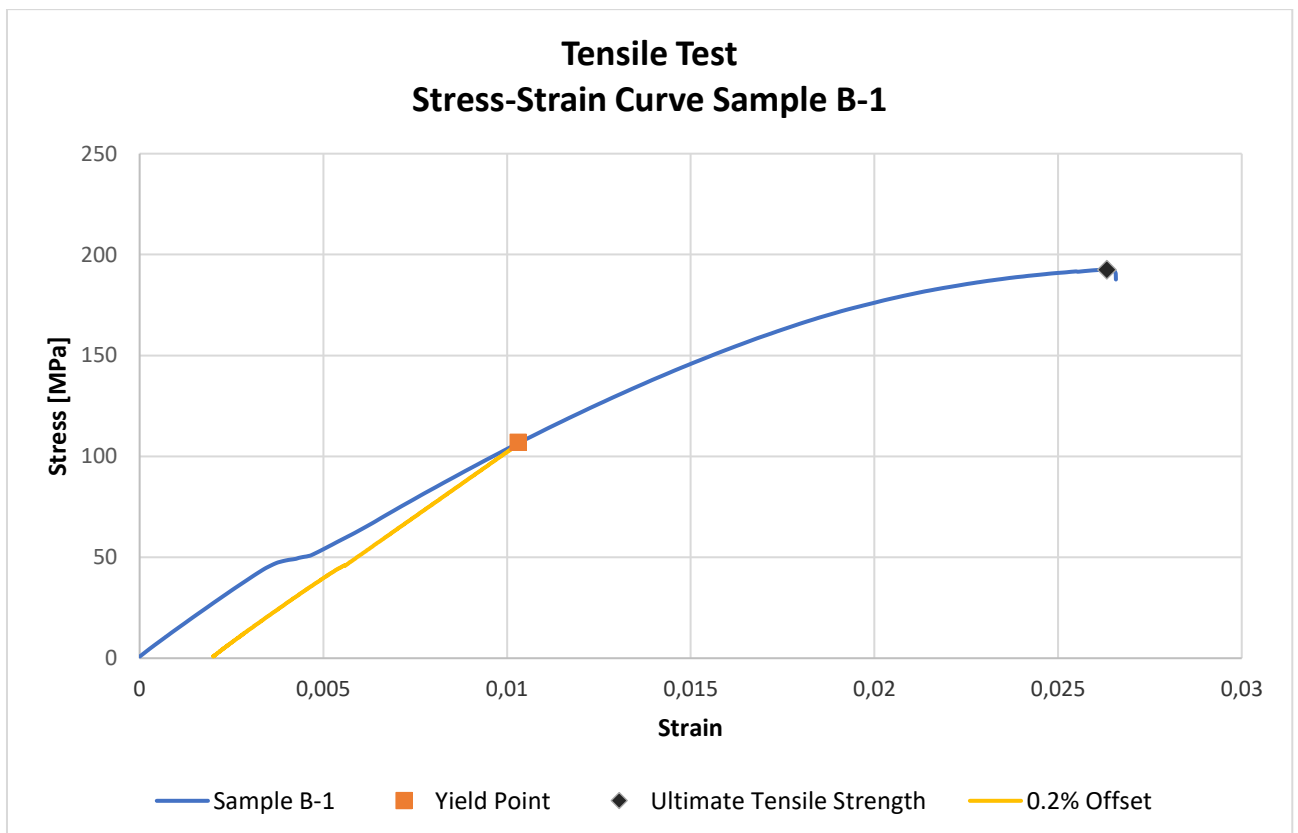


Figure 46. Stress-strain curve of tensile test sample B-1

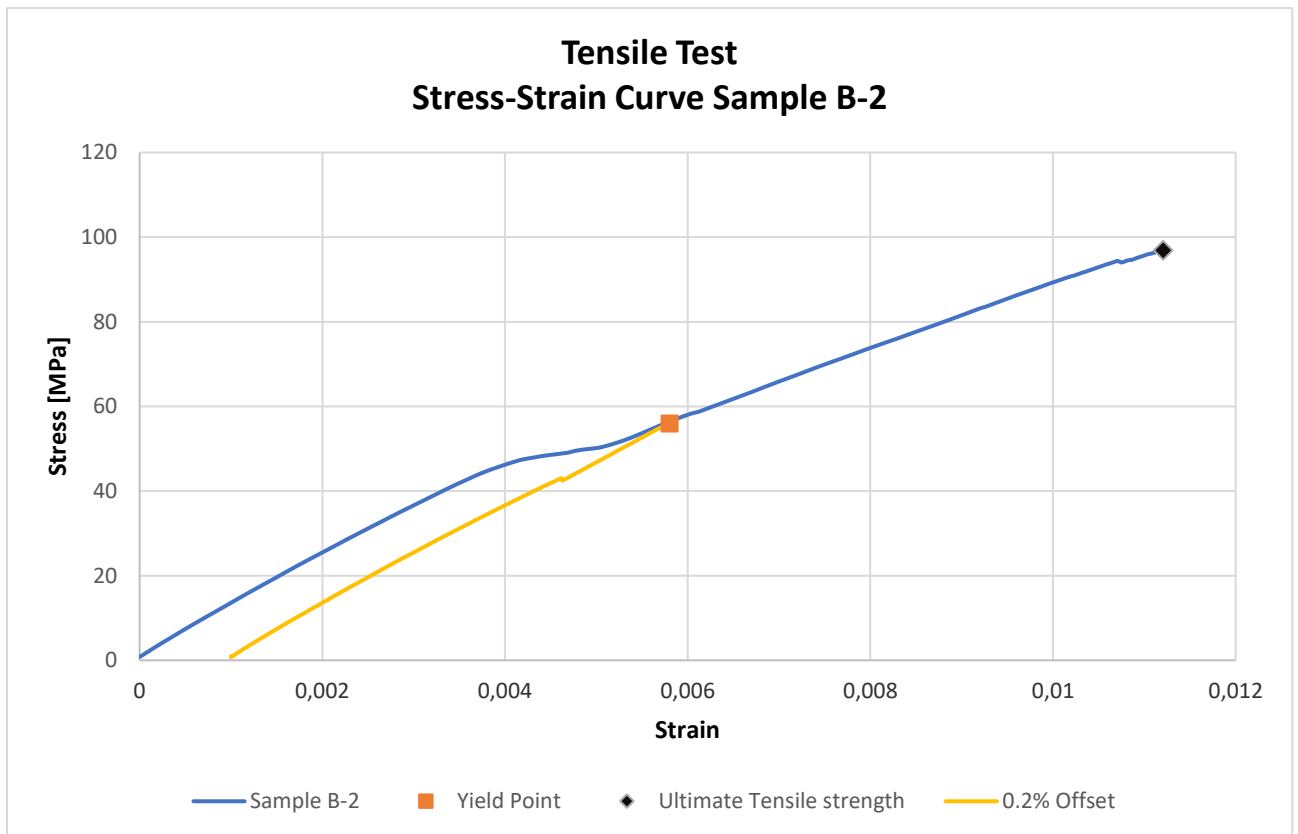


Figure 47. Stress-strain curve of tensile test sample B-2

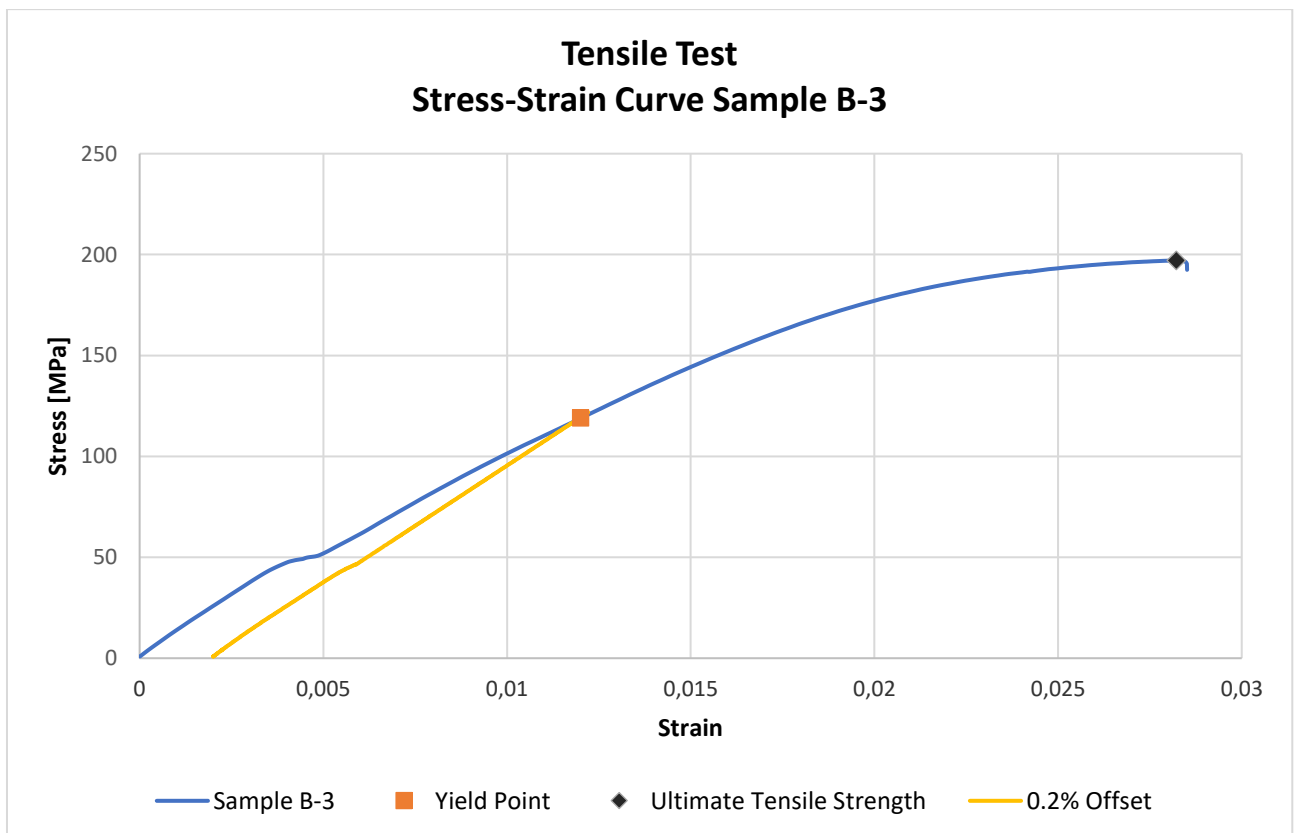


Figure 48. Stress-strain curve of tensile test sample B-3

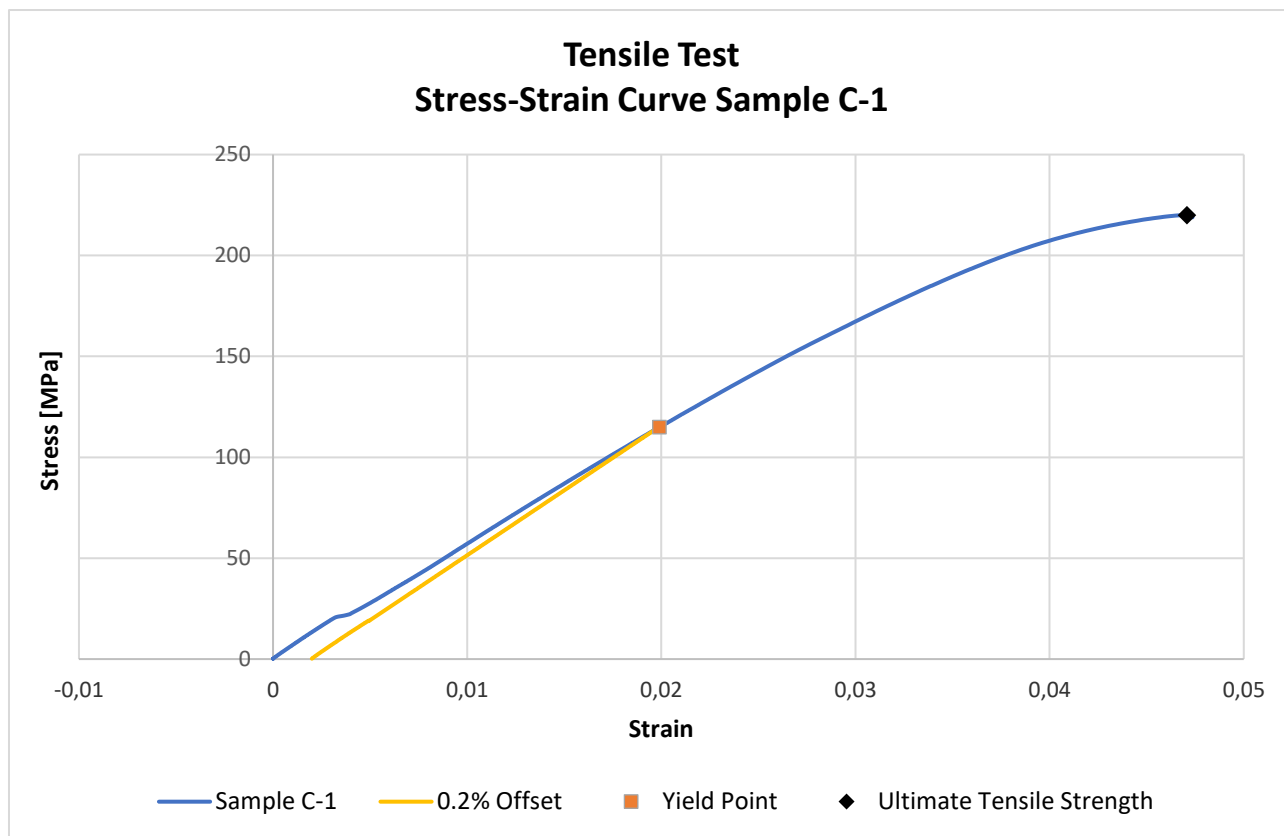


Figure 49. Stress-strain curve of tensile test sample C-1

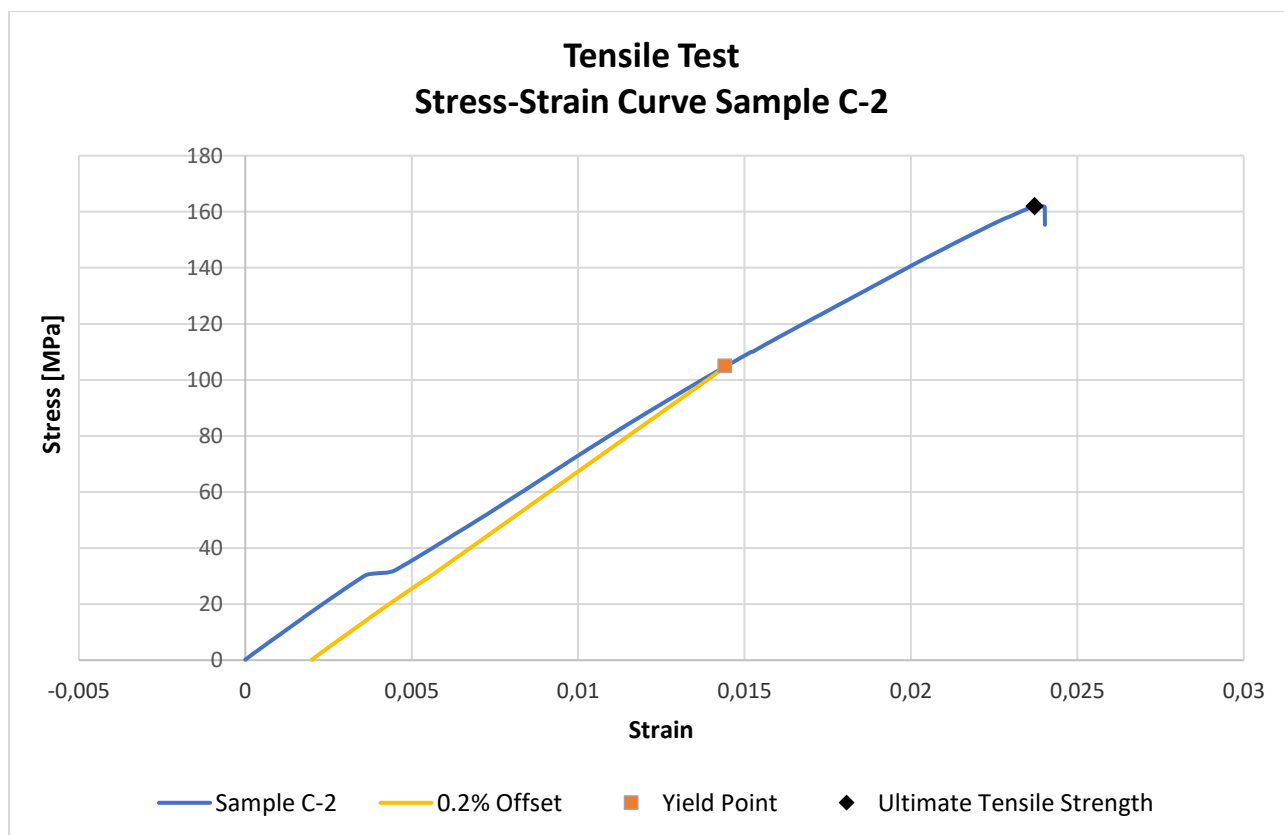


Figure 50. Stress-strain curve of tensile test sample C-2

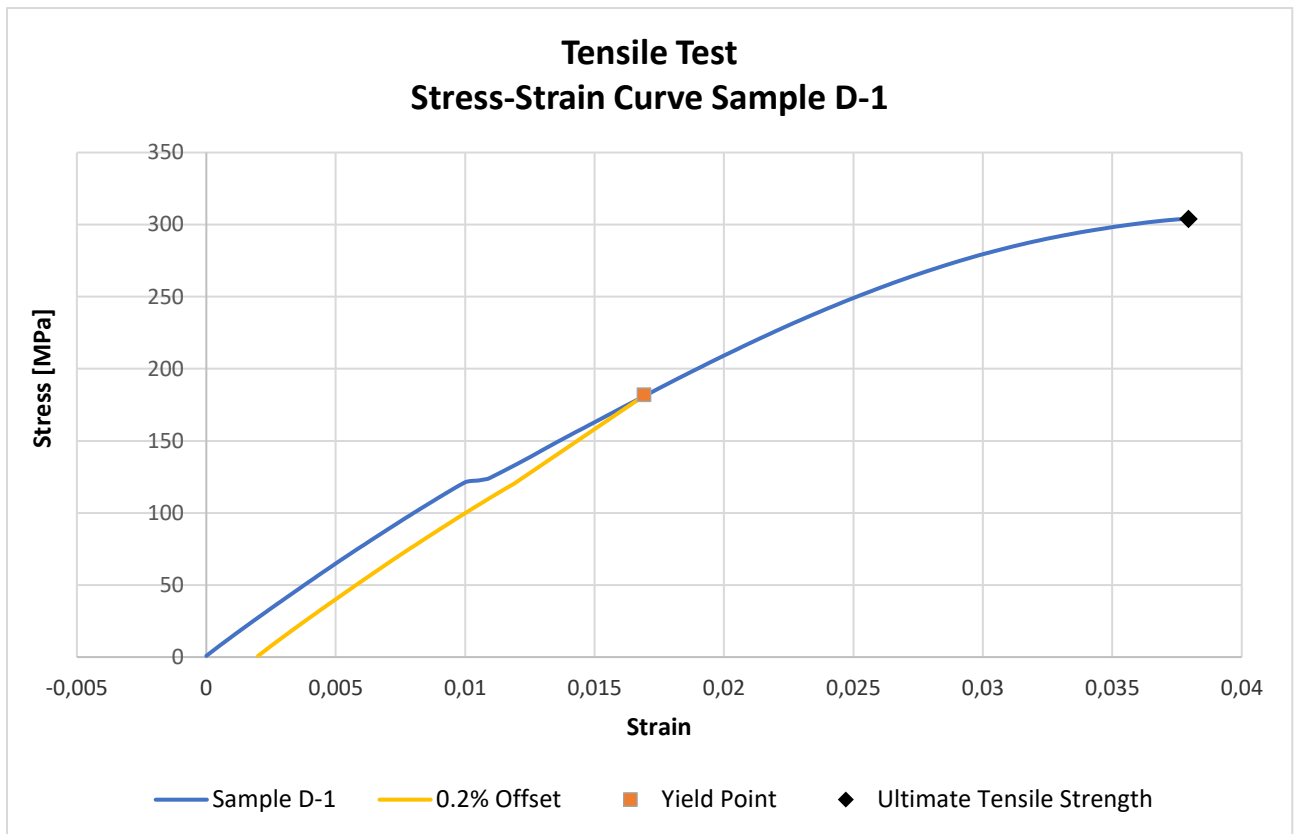


Figure 51. Stress-strain curve of tensile test sample D-1

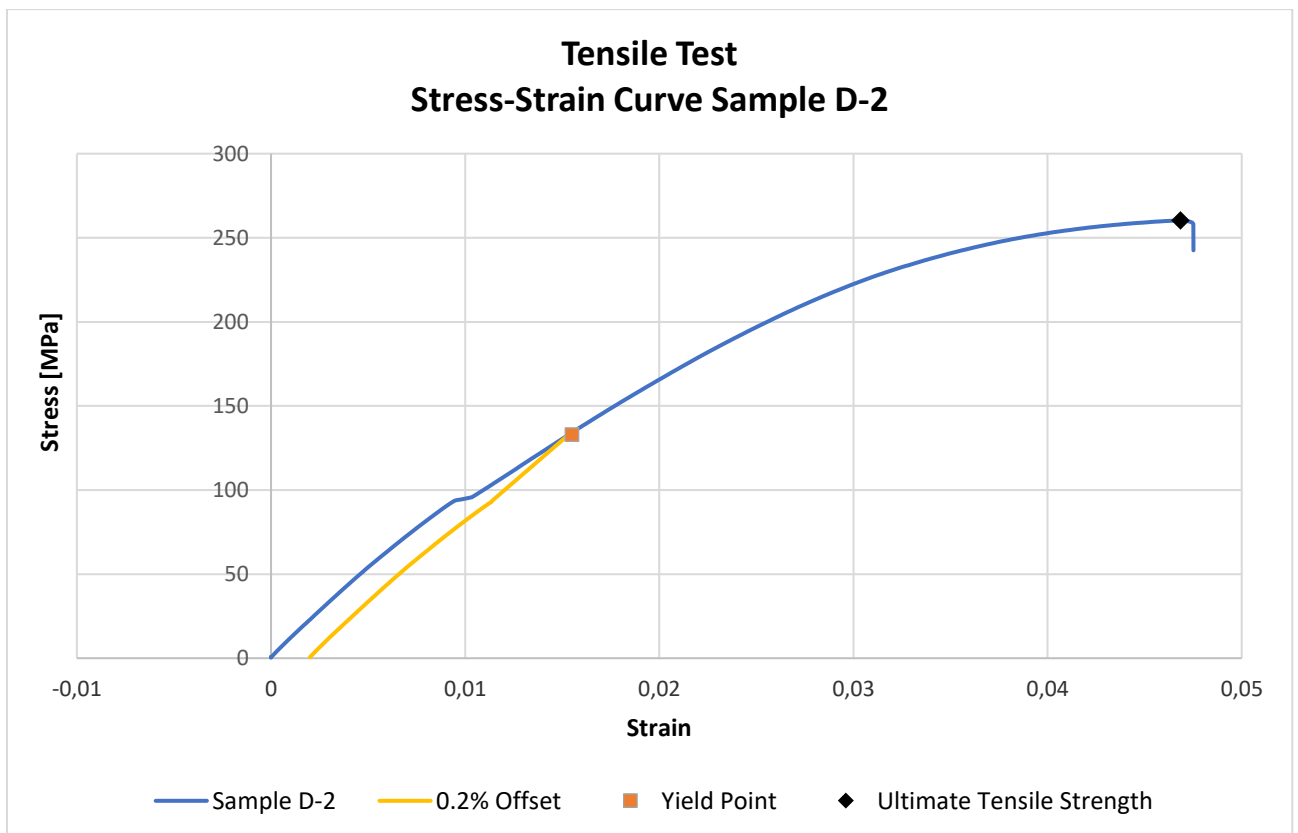


Figure 52. Stress-strain curve of tensile test sample D-2

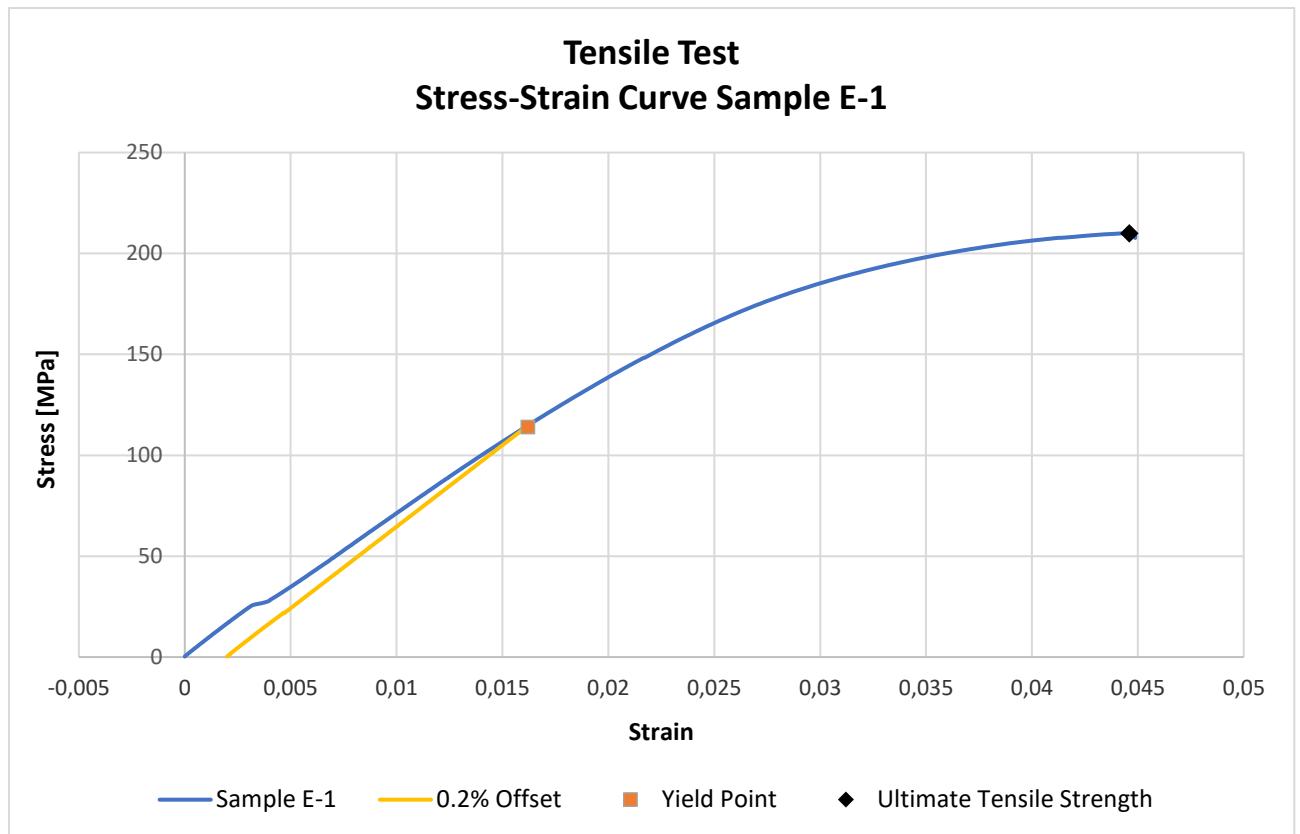


Figure 53. Stress-strain curve of tensile test sample E-1

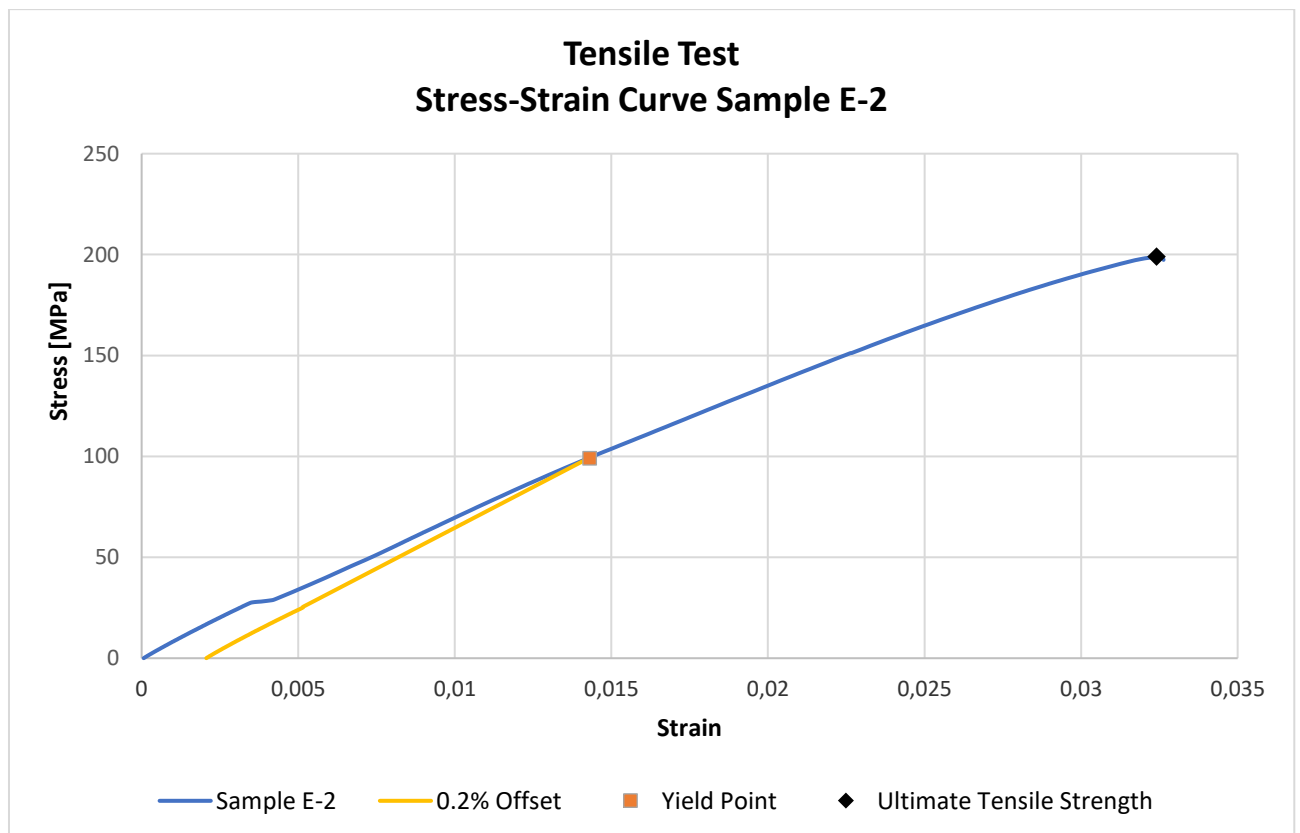


Figure 54. Stress-strain curve of tensile test sample E-2

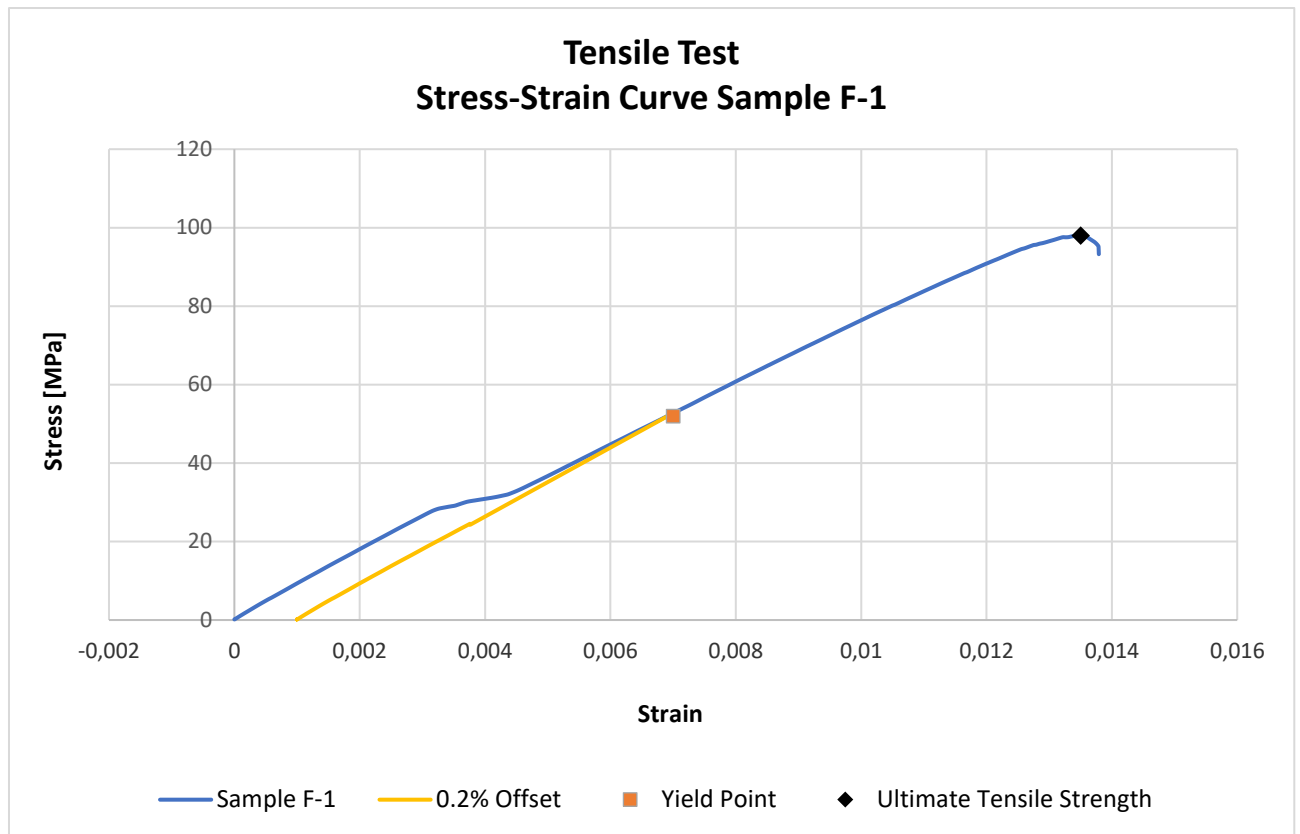


Figure 55. Stress-strain curve of tensile test sample F-1

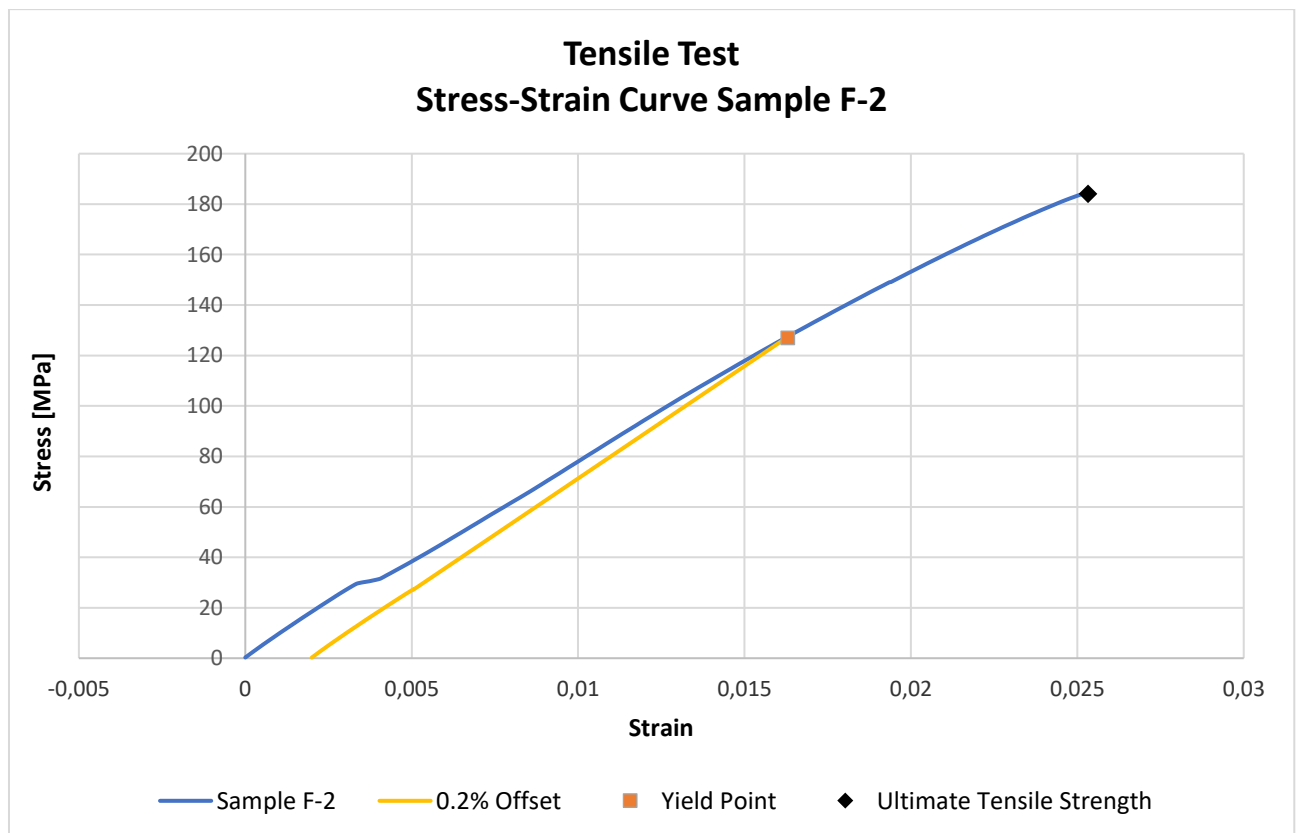


Figure 56. Stress-strain curve of tensile test sample F-2